Multifunctional Electrospun Nanofibers Incorporated with an Anti-infection Drug and Immobilized with Proteins

By

Shufei Zhou

A Thesis

Submitted to the Faculty of Graduate Studies in Partial Fulfillment of the Requirements for the Degree of

Master of Science

Department of Textile Sciences

University of Manitoba

Winnipeg, Manitoba

Copyright © 2010 by Shufei Zhou

Abstract

Electrospinning has been used to fabricate ultrafine fibers with sizes ranging from nano to micrometers. Nanofibers electrospun from biocompatible and biodegradable polymers have been extensively investigated for their potential applications in wound healing and tissue regeneration. These nanofiber materials can be modified to incorporate bioactive molecules, such as antibacterial agents that provide infection control, or functional proteins which promote cell proliferation and tissue reconstruction. Despite the numerous studies on the development and design of nanofibers for biomedical applications, there has been little research on multifunctional nanofibers that are incorporated with both antibacterial drug(s) and bioactive proteins. The objective of the current study is, therefore, to develop nanofibers that are functionalized by several bioactive molecules.

In this study, electrospinning was utilized to fabricate nanofibers from biodegradable polymers PLLA (Poly-L-lactide) and the copolymer PLLA-PEG (Polyethylene glycol)-NH_2.A water soluble antibiotic drug, Tetracycline Hydrochloride (TCH), was incorporated into the electrospun nanofibers via emulsion electrospinning. The TCH-loaded nanofibers were surface modified to produce functional groups that can be further conjugated with a model protein, Bovine Serum Albumin (BSA).Drug releasing profiles of the medicated nanofibers were monitored and their antimicrobial properties were evaluated. Proteins (BSAs) immobilized on the fiber surface were verified by ATR-FTIR. The number of immobilized BSAs was determined using a UV-Vis spectrophotometer. The results of the study suggested that this multifunctional nanofibrous material could be a promising material for wound dressing or scaffolds for tissue engineering.

Acknowledgments

The author wishes to express a special thank-you to her advisor, Dr. Wen Zhong, for her patient guidance and encouragements throughout the study.

Special thanks are also extended to thesis committee members: Dr. Song Liu, Department of Textile Sciences, and Dr. Yuewen Gong, Faculty of Pharmacy, for their professional suggestions on the thesis and experiments.

The author would also like to thank Faculty of Chemistry and Faculty of Food Sciences for providing lab spaces and equipments.

Table Of Contents

List Of Tables

List Of Figures

Chapter 1 Introduction

1.1 Background

Electrospun nanofibres with biocompatible and biodegradable polymers have been used as wound dressings or scaffolds for tissue engineering because of their larger surface to volume ratios, porous structures, and excellent mechanical strengths. They simulate the extracellular matrix (ECM) to provide an appropriate biological environment for cell growth and tissue regeneration. Electrospinning can produce fibers with diameters that range from tens of nanometers to hundreds of micrometers. These nanofibrous meshes may provide platforms not only for viable cells to form functional tissues, but also for bioactive molecules to control infection and/or to regulate/promote cell proliferation and tissue regeneration. Therefore, incorporation and/or immobilization of bioactive molecules in/onto nanofibers has become an emerging topic. This gives rise to the question of how to enhance biodegradable nanofibers' capacity to incorporate and immobilize bioactive molecules like proteins, enzymes, growth factors, anitibodies, DNA, etc.

Extensive work has been carried out on the development of functional nanofibers for wound care or tissue engineering. A large number of drugs have been incorporated into nanofibers of different compositions. These drugs include model drugs [1], anti-inflammatory drugs [2],and anticancer drugs [3, 4]. It has been reported that these drug-carrying nanofibers could provide sustained release of drugs over time, and therefore enhance efficacy of drugs[5]. There are also numerous studies concentrated on

incorporation of bioactive proteins onto/into nanofibers. These proteins can be model proteins, enzymes, growth factors, etc[6-12]. Many of these bioactive proteins-loaded nanofibers have been shown to enhance cell proliferation and/or tissue regeneration, therefore, they may be useful in biomedical applications.

Although there has been a fair amount of research in nanofibers that focus on functionality of bioactive molecules, there has not been much work on the development of multi-functional nanofibers which incorporate both anti-infectious drugs and functional proteins. Nevertheless, such functions are desirable for the nanofibers' applications in wound care or tissue regeneration to provide both infection control and promotion of wound healing or tissue regeneration. The present study, therefore, aims to develop such multi-functional nanofibers. Specifically, a model antibiotic, Tetracycline hydrochloride (TCH) was loaded into the PLLA/PLLA-b-PEG nanofibrous mat via emulsion electrospinning. The drug-loaded nanofibers were then surface-modified to allow a model protein, Bovine Serum Albumin (BSA) to be covalently immobilized onto the nanofiber's surface. BSA labeled with two different fluorescence dyes were immobilized onto the nanofiber surface respectively via two different functional groups on the fiber surfaces. Then the multi-functions of the developed nanofibers were verified by microorganism susceptibility tests and fluorescence microscopic images. These nanofibers are potentially useful for wound care and tissue engineering scaffold.

1.2 Objectives

The objectives of this study are to incorporate a hydrophilic drug inside of the electrospun nanofibers and to investigate the surface functionalization of biodegradable

and biocompatible polymers that may enhance their capacity to immobilize bioactive molecules. The specific aims of the study are:

1. To incorporate a hydrophilic antibiotic (Tetracycline Hydrochloride) into electrospun nanofibers by emulsion electrospinning and to test sustained drug release from the nanofibers;

2. To investigate methods that modify surface functionality of drug-loaded nanofibers to enhance their capacity to immobilize proteins onto the surface of electrospun nanofibers. Bovine Serum Albumin (BSA) will be used as a model protein in this research;

3. To confirm the bioactivity of antibiotic drugs on the nanofibers by examining the antimicrobial ability of drug-loaded nanofibrous mats.

1.3 Components of the thesis

This thesis is composed of 5 chapters. Chapter 1 briefly introduces the background and objectives of the research. Chapter 2 will be a comprehensive literature review on related research, including history and development of electrospinning, natural and synthetic polymers used for electrospinning, different methods to incorporate drugs into nanofibers, and ways of immobilizing bioactive molecules onto nanofibers. Chapter 3 describes materials, equipment and detailed procedures to load TCH into nanofibers and to immobilize BSA onto fiber surface. Chapter 4 demonstrates results of material development and characterization, including drug release profiles,

validations of immobilized proteins on drug-loaded nanofibers, and antibacterial efficiency test of functional nanofibers. Chapter 5 provides a conclusion to this study and offers some thoughts on future work.

Chapter 2 Literature Review

This chapter is a comprehensive literature review on research related to this study. It starts with a brief introduction to wound dressings and follows with a history of electrospinning and its advantages in tissue engineering and wound care. Development of electrospinning apparatus and polymers used for electrospinning will be covered. Previous studies on nanofibers loaded with drugs and/or immobilized with bioactive molecules will also be discussed.

2.1 Wound dressings

The wound healing process usually includes three phases: inflammatory phase, fibroblastic phase and maturation phase [13-15]. The inflammatory phase begins immediately after wounding and lasts about 4 days. The goal of this phase is hemostasis, detachment of deteriorated tissue and wound cleansing[13, 15]. The fibroblastic phase appears at the end of inflammatory phase and is dominated by cell proliferation to replace damaged tissue. It lasts about 3 weeks [16, 17]. The final phase of wound healing is the maturation phase, which includes tissue regeneration for maturation, scar formation and epithelialisation[18]. During such processes, wound dressing is an important factor in the non-surgical treatment of wounds. It provides a barrier against microorganisms, dirt and other hazards. It also protects wounds against further injury and abrasion by acting as a cushion.

Wound dressings first appeared as grease-soaked gauze bandages in ancient Egypt [19]. Over thousands of years, wound-care materials have become more sophisticated, but their primary functions for wound healing remains the same. Traditional wound dressings, such as cotton gauze, have good adsorption and are soft to the touch, but they

can be overly permeable, non-occlusive and easy to dry out. These features may lead to wound adherence and cause pain during removal. In particular, capillary loops (i.e. granulation tissue) can grow into dressing structures, thereby resulting in dressing adherence [20]. Such adherence leads to wound trauma, which is often noted with bleeding during dressing removal.

Modern wound dressings are multilayer dressings containing 1)a low adherent primary dressings which allow easy removal and appropriate moisture transportation to maintain proper moisture level;2) a second absorbent layers which can absorb blood and body fluids; however, these layers should not be too absorbent or they may cause primary dressings to dry out too quickly. Alginate fibers, derived from seaweed, can be used as primary dressings for their biocompatibility and biodegradability. They can absorb moderate to high levels of exudates and when in contact with exudates, they form a hydrophilic gel which conforms to wound surface and acts as a hemostat. However, if they become supersaturated in their gel transformation, they may cause maceration of surrounding skin or strikethrough of excess exudates through any secondary dressing. If a wound is too dry to transform an alginate fiber into a hydrogel-like material, then the wound surface will remain dry and un-dissolved fibers do not provide moist and interactive healing[21].

Since the discovery of wound re-epithelialization and healing can be faster under occlusion dressings, occlusive dressings have become a standard for wound treatment[17]. It is also recognized that healing process can be further enhanced by wound dressing materials that can release beneficial bioactive agents such as drugs and proteins, because proteins like growth factor and fibrin are needed for collagen synthesis

in wound site [16]. Jiong, Han et.al. compared absorbency and permeation of four dressings on burn wounds: carbon fiber dressing, hydrogel dressing, silver nanoparticle dressing and Vaseline gauze. Results showed that carbon fiber dressing had the highest absorption and evaporation rate from burn wounds [22].

Recently, electropun nanofibers have been extensively studied for development of innovative dressing materials for wound healing. Characteristics required for wound dressings include mechanical integrity, temporization of adherence to a wound, the ability to facilitate temperature homeostasis and allow gas exchange, and absorbance of exudates. All of these characteristics for wound dressing can be provided by electrospun nanofiberous mats [23]. Current commercial available skin substitutes are made up of fibroblasts or keratinocytes on collagen scaffolds, whose structural heterogeneity is generated by freeze drying. Powell et.al. have compared freeze drying and electrospun nanofibrous skin substitutes in term of cell distribution, proliferation, organization, engraft maturation and wound healing[24]. Results showed no significant differences in cell proliferation, surface hydration and cellular organization between the two skin substitutes; however, wound contraction was reduced with electrospun collagen nanofibrous scaffold. This may suggest an advantage of reduced morbidity in patients treated with skin substitutes made from electrospun collagen nanofibrous scaffold.

Collagen nanofibrous mats have shown great wound healing properties. In twin full-thickness rectangular back wounds in a rat model, microscopic examination revealed that early-stage healing in the collagen nanofiber group was faster than that in the cotton gauze control group. The wound surface of the control group was covered with fibrinous tissue debris, overlying a dense infiltration of polymorphonuclear leukocytes and

proliferating fibroblasts. However, in the collagen nanofiber group, no surface tissue debris, prominent capillaries and fibroblasts proliferation were observed. Moreover, late-stage healing process in the control group was similar to that of the collagen nanofiber group. Furthermore, wound epithelialization was complete after 4 weeks in both groups [25].

Chitin and chitosan have been used in a variety of biomedical applications, such as materials to promote bone regeneration in tissue engineering, and/or sutures. They have also been used as dressing materials for wound healing. The results of research showed that chitosan can regulate wound healing processes like fibroplasias and reepithelialisation [26]. It is suggested that chitosan has unique haemostatic properties [27] and can modulate the migration of neutrophils and macrophages, which would subsequently regulate wound repair processes such as fibroplasias and reepithelialisation [28, 29]. It has also been reported that chitin and its derivatives could accelerate tensile strength of wounds by speeding the synthesis of collagen [30, 31]. It was found that electrospun collagen/chitosan composite nanofibrous membrane has better wound healing rate than gauze and commercial wound dressings in an animal model [32].

Other polymers were also used in the development of electrospun nanofibrous dressing materials. It was reported that electrospun polyurethane nanofibrous dressings can control evaporative water loss, allow oxygen permeability, and enhance drainage of wound fluid due to its high porosity. Polyurethane nanofiberous dressings was also found to promote wound healing compared with commercial permeable polyurethane wound dressings because of their adherence to wet wound surfaces, absorption of exudates, and

increased epithelialization rates[33, 34]. Silk fibroin [35]and poly-vinyl alcohol[36] were also studied for their applications in nanofibrous dressing.

Antibacterial agents have been incorporated into nanofibrous dressing materials to provide an anti-infection capacity. The silver nanoparticles were reported to demonstrate inhibition against Gram-positive Staphylococcus aureus (ATCC 6538) and Gram-negative Escherichia coli (ATCC 25922). Silver (Ag+)-zirconium phosphate nanoparticles have been incorporated into electrospun nanofibers for developing functional wound dressing materials. Rujitanaroj et.al. developed gelatin nanofibrous mats containing silver nanoparticles (nAg) with antibacterial activity. The nAg-loaded gelatin nanofibrous mats were then crosslinked to improve their stability in aqueous solutions. The antimicrobial capacity of the nanofibers were verified by testing against Pseudomonas aeruginosa, E-coli and some other common bacteria found on burn wounds [37]. Xu and Zhou also tested nAg containing electrospun gelatin nanofibers against Staphylococcus aureus and Pseudomonas aeruginosa [38]. Wound dressing material was also prepared by electrospining of (PVA)/AgNO3 aqueous solution into non-woven webs which is then treated with heat or UV radiation to reduce the Ag+ ions in the electrospun PVA/AgNO3 fiber web into the Ag nanoparticles.[39]. Ag nanoparticles were proved to have excellent antibacterial ability since Ag can interact with enzymes and proteins important for bacterial resporation, and interacts with bacterial DNA, therefore inhibiting cell division. Silver nanoparticles were also impregnated into bacterial cellulose. Bacterial cellulose is synthesized by the acetic bacterium: Acetobacter xylinum. The fibrous structure of bacterial cellulose consists of a three-dimensional non-woven network of microfibrils, The resulted materials not only provided a moist environment

but also exhibited antimicrobial ability against both Gram-negative and Gram-positive bacteria [40]. Duan et.al. produced antimicrobial nanofibers of poly(ε-caprolactone) (PCL) by electrospinning of PCL solution with silver loaded zirconium phosphate nanoparticles. The antimicrobial tests showed that the nano-AgZr loaded PCL nanofibers have strong antimicrobial abilities against Staphylococcus aureus and Escherichia coli. To evaluate the biocompatibility of the nanofibers as potential wound dressings, primary human dermal fibroblasts (HDFs) were cultured on the PCL nanofibrous mats. The results indicated that cells attached and proliferated as continuous layers on the nano-AgZr loaded nanofibers, and maintained a healthy morphology [41].

2.2 Introduction of Electrospinning

2.2.1 History of Electrospinning

The technique of producing fibers by electrostatic force, known as electrospinning, can be traced back to the 1930s when Formhals patented his invention of the process and the apparatus for producing polymer filaments using electric charges[42]. In Formhal's eletrospinning process, a movable thread collector was used to collect threads in a stretched condition. In the earliest years, conventional fibers of relatively large diameters were produced by pulling molten polymer out through a mold. The polymer was then let dry to form individual fibers [43]. In Formhal's invention, threads were aligned parallel onto a collecting device. Instead of any external mechanical force, an electric field was applied to extend a stretching force on polymer fluid. The first electrospinning method introduced by Formhals had some drawbacks: the distance between spinning nozzle and fiber collecting device was too short for fibers to get completely dry before hitting

collecting device. Formhal later refined electrospinning process by increasing nozzle-collecting device distance [44]. In 1940, Formhal created another method for producing composite fibers by electrospinning multiple polymer fibers onto a moving substrate [45]. Following Formhal's methods, a series of electrospinning trials have been carried out by a number of researchers. The best shape of polymer jet adjacent to spinning nozzle was found to be a cone by Taylor in 1969[46]. This cone was later referred by other researches as the "Taylor Cone". The cone is very important since it defines the onset of extensional velocity gradient in fiber forming process [47].

There were also extensive researches that focus on the relationship between fiber morphology and electrospinning parameters. Baumgarten [48] reported that fiber diameter depended on viscosity of polymer solution. According to Larrondo and Mandley, fiber diameter reduced by 50% when applied voltage doubled. This indicated an important role of applied voltage on fiber characteristics [49-51]. The stability of jets was also studied and it was shown that unstable jets produced the fibers with wider diameter distributions [52].In 1995, Reneker and Chun[53] found that jet diameter decreased with the increase in its distance from the cone apex. In their studies on characteristics of polyethylene oxide (PEO) nanofibers, they also found that PEO solution with viscosity less than 800cP was too dilute to form stable jet, while the solution with viscosity more than 4000 cP was too thick to form fibers. In 1996, Reneker and Chun stated that the electrospun fibers are subjected to a group of forces including tensile, gravitational, aerodynamic, rheological, and inertial forces [54]. The influence of applied voltages on the shape of electrospun nanofibers was studied by Deitzel [55, 56]. The studies showed that an increase in the applied voltage changes the shape of jet

surface and increase the bead defects. Gibson et. al. indicated that nanofibrous mats have very little resistance to the moisture vapor diffusion[57]. Studies focused on solvent volatility were also conducted to understand the production process of electrospun nanofibers[58, 59]. Results showed that solvent plays a major role in the formation of nanostructure by influence the phase separation process.

2.2.2 Electrospinning Process and Apparatus

2.2.2.1 Electrospinning Apparatus

Generally, an electrospinning apparatus is composed of a high voltage electric source with positive or negative polarity, a syringe pump which delivers solution from a syringe to a spinnerette or needle, and a conducting collector (Figure 2.1). The collector can be made into any shape, such as a flat plate or a rotating drum, depending on the desired alignments of fibers on the collector [60-62]. For example, using a rotating drum as the collector can produce partially aligned fiber. In the process of electrospinning, a high voltage is applied to a polymer solution and charges are induced within the polymer solution. In order to carry out electrospinning, charges on polymer solution must be high enough to overcome surface tension of the solution. When charges within the solution reach to a critical amount, a jet will erupt from polymer droplet at the tip of needle to form a Taylor cone. The electrospinning jet then travels towards collector and forms fibers with diameters in micron or nano meters.

Figure 2.1 Electrospinning setup [63]

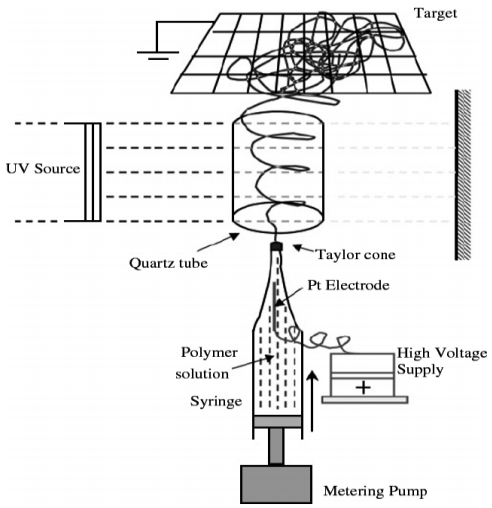

2.2.2.2 Processing parameters of electrospinning

Processing parameters can affect morphology of electrospun nanofibers. These parameters include polymer solution parameters, applied voltage, temperature, distance between needle and collector, etc.

Electrospun nanofibers can be processed from molten polymers [64, 65]. However, most of recent reports on nanofibers produced electrospinning fibers from polymer solutions. The properties of polymer solutions, including viscosity and surface tension, have significant effect on electrospinning process and fiber morphology. According to Shenoy et. al. [66], the viscosity of a solution made by the polymer of high molecular weight is higher than that of a solution of made by lower molecular weight. They also found that polymer chain entanglements have a significant impact on whether jet breaks into droplets and results in electrospun fibers containing beads. During the stretch of solution, the entanglement of polymer chain prevents electrically driven jet from

breaking up. Besides, viscosity should not be too high to dry out solution at the tip of needle [67], so as to make it difficult to pump solution through needle [68].

The higher surface tension of polymer solution, the greater tendency for the solvent molecules to congregate and the lesser interaction between solvent and polymer molecules when the solution is charged [43]. Solvent with low surface tension can be added into solution to form smooth fibers [43]. Also It has been tried that surfactant was added into polymer solution to reduce surface tension and yield uniform and bead-free nanofibers [69, 70].

The voltage applied to solution is also an important parameter in electrospinning. The high voltage will initiate electrospinning process where the electrostatic force in solution overcomes surface tension. It has been reported that in most cases a higher voltage will lead to greater stretching of solution and smaller diameter of the fibers [71, 72]. However, at a lower voltage, the slower acceleration of jet and the weaker electric field may increase the flight time of the jet which favors formation of finer fibers [43].

The distance between tip of needle and ground collector will also have impact on the fiber morphology. For example, when the distance between tip and collector is reduced, the jet has less time to travel before it reaches the collector. As a result, there is not enough time for solvent to evaporate when it reaches the collector. On the contrary, if there is a longer distance between tip and collector, which means a longer flight time for solution to be stretched before it reaches the collector, the electrospun nanofibers diameter will increase [72]. The change of fiber diameter with different distance between tip and collector may be due to the decrease in electrostatic field strength [73].

2.2.2.3 Improvements and modifications in Electrospinning Apparatus

During electrospinning process, nanofibers are usually collected in a random fashion. However, in tissue engineering, scaffolds with aligned fibers are sometimes more desirable to guide cell proliferation [6, 74]. Patel et.al.[6] found that aligned nanofibers significantly induce neurite outgrowth and enhance skin cell migration during wound healing compared to randomly oriented nanofibers. Xu et.al. investigated PLA-PCL nanofibrous scaffold with aligned fibrous structure and found that human coronary artery smooth muscle cells (SMCs) attached and migrated along the axis of aligned nanofibers, and expressed a spindle-like contractile phenotype [75]. Zong et. al. investigated structural and functional effects of oriented electrospun scaffolds on cardiac myocyte proliferation[76, 77]. They found that the oriented nanofibrous matrix allows cardiomyocytes to make extensive use of provided external cues for isotropic or anisotropic (oriented) growth, and to some extent to crawl inside and pull on fibers.

Mo et.al.[78] used an auxiliary electrode with a sharp edge and a negative charge to guide fiber deposition on a mandrel. They found that when the sharp edge bar was vertical to the rotating axle of mandrel and just beneath spinning nozzle, nanofibers with circumferential alignment can be obtained.

Several ways to collect aligned nanofibers have been developed, including: 1) to provide an auxiliary electrical field[79-81], 2) to use a grounded wheel collector or a rotating grounded mandrel[80-82], 3) to apply uniaxial or biaxial stretching [83, 84]. It was reported that porosity of nanofibrous scaffold decrease with increase in stretching extension [72].

Kidoaki et. al. introduced two new electrospinning techniques [85]: multilayer electrospinning and mixed electrospinning. In multilayer electrospinning, each polymer was electrospun individually, collected on the same collecting device and overlapped to one another. This fiber mesh can be used for artificial blood vessel scaffold. By multilayer electrospinning, a hierarchically ordered structure consisting of different polymer meshes could be obtained. In mixed electrospinning, two different polymers were electrospun simultaneously from different needles under different conditions; however, the fibers were mixed on the same collector and form a mixed nanofiber mat.

Co-axial electrospinning can produce core-sheath bi-component nanofiber structures. In co-axial electrospinning process, two dis-similar polymers are delivered independently through a co-axial capillary and drawn to generate nanofibers in core-sheath configuration [86, 87]. The advantage of using co-axial electrospinning is that it can produce core materials that will not form fibers via electrospinning. The outer shell polymeric material will serve as the template. This co-axial electrospinning can be used to produce materials for drug delivery and photocatalysis[9, 10].

2.2.3 Material Class

A large number of polymers have been electrospun to form nanofibers. Generally they can be divided into two categories: synthetic polymer and natural polymer.

Natural polymers usually exhibit good biocompatibility and low immunogenicity, which enable them to be used in biomedical areas. Many natural polymers like proteins, DNAs [88] and lipids have been fabricated into nanofibers. Protein fibers, mainly made

from collagen, gelatin, elastin and silk fibroin, have been well studied in recent years [37, 89, 90].

Collagen is the most widely used natural polymer in electrospinning because it is the most abundant protein in human body. It is found throughout the interstitial spaces, and provide overall structural integrity and strength to tissues. More importantly, collagen structure provides cells with appropriate biological space for embryologic development, organogenesis, cell growth, and wound repair. Natural polymer of collagen is principal structural elements of extracellular matrix (ECM) [91]. Electrospun collagen mats may be a biomimicking scaffold when sub-micron fibers possessing natural collagen ultra structure can be created. Collagen type II was electrospun for use in cartilage tissue engineering by Matthews et. al. [92]. Human articular chondrocytes seeded onto electrospun collagen type II scaffolds were shown to migrate into the scaffold.

Elastin is a protein in connective tissues which is elastic and allows tissues to resume their shape after stretching. The skin contains thin strands of elastin that help to keep it smooth [76]. Researches show that elastin is extremely effective as a tissue scaffold or graft, particularly in vascular applications [93].

Silk fiber is another natural protein material that has outstanding mechanical properties. Electrospun nanofibers from silk fibroin (SF) have good biocompatibility, oxygen and water vapor permeability and biodegradability. In addition, it induces minimal inflammatory reaction [94]. It was found that normal human keratinocytes and fibroblasts seeded on SF nanofibers were able to attach and grow, indicating that SF nanofibers may be a good material for wound dressing and tissue engineering scaffold[95, 96].

Synthetic polymers often offer many advantages over natural polymers. Firstly they can be tailored in a wider variety of properties such as fiber diameter, hydrophobicity, hydrophilicity and biodegradability. Secondly, synthetic polymers may be of low costs and therefore represent a more reliable source of raw materials. Typical synthetic polymers used in biomedical applications include hydrophobic biodegradable polymers, such as polyglycolide (PGA) [97, 98]. polylactide (PLA) [99-102], and poly(ε-caprolactone) (PCL) [103-105]. Other hydrophilic biodegradable polymers like polyurethane [106], poly(vinyl alcohol) [107, 108] and poly(ethylene oxide)[109] have also been electrospun into nanofibrous scaffold for biomedical applications.

Copolymer or physical mixing of two polymers was also used in electrospinning [110-112]. There are two types of copolymers: random copolymers and block copolymers. In a random copolymer, two monomers distribute in random sequences, which can exhibit properties that is intermediate between the two monomers. However, in a block copolymer, homopolymers are repeated alternatively, which will show properties of each homopolymer [43]. In polymer blends, the polymers tend to separate into distinct phases due to incompatibility, and the links between different polymers are not strong because no chemical reactions are involved in blending. The use of copolymers can generate new materials for desirable properties. For example, biodegradable hydrophobic polyesters generally have good mechanical properties but lack cell affinity for tissue engineering. The incorporation of a proper hydrophilic polymer segment can increase the cell affinity.

Natural polymers usually possess weak mechanical properties; however, blending of natural and synthetic polymers can overcome this problem by improving mechanical strength, durability, and cell affinity. Kwon et.al. electrospun poly(L-lactide-co-epsilon-

caprolactone) (PLCL) with type I collagen using 1, 1, 1,3,3,3-hexafluoro-2-propanol (HFIP) as a solvent. An increase in collagen content in the solution was shown to decrease the mean diameter of fibers. Human umbilical vein endothelial cells (HUVECs) were highly elongated and well spread on this fibrous surfaces [111]. The mixture of heparin and PEG was also electrospun to prepare nanofibrous scaffolds [113]. It was showed that the presence of PEG in the electrospun scaffolds prolonged the release of heparin, which could closely match the time scale needed for use in wound dressings.

2.3 Physical and Chemical Properties of PEG and PLAand Their Applications

Poly(lactide) (PLA) is a biodegradable aliphatic polyester that is very popular for use in medical applications. Chemistry of PLA involves processing and polymerization of lactic acid monomer. Lactic acid (CH3CH(OH)COOH) is a simple chiral molecule which exists in two enantiomers, L- and D-lactic acid, differing in their effect on polarized light [114]. Polymerization of lactic acid into high molecular weight PLA can be achieved by condensation (Fig 2.2). The methyl group in the monomer makes PLA more hydrophobic than PGA; it also presents a steric hindrance that gives PLA a higher solubility in organic solvents and significantly slows hydrolysis; otherwise PLA typically degrades within 30 to 50 weeks. PLA also has a moderate crystallinity (about 37%) but a lower melting point (96 °C) [115]. PLA has been electrospun into nanofibers from its solution in chloroform, methylene chloride, dimethylformamide (DMF), etc [116].

Fig2.2 Synthesis of polylactic acid [114]

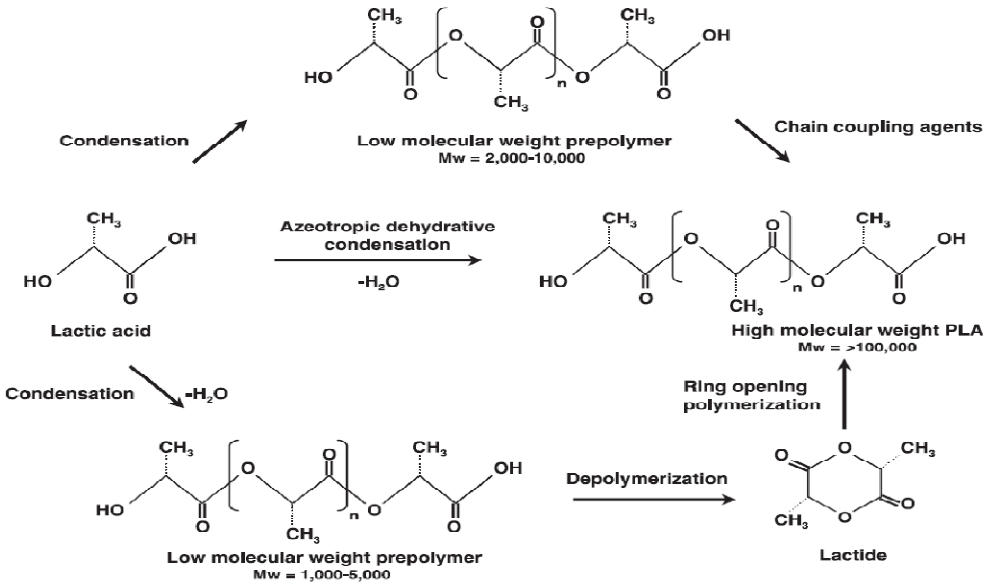

PLA has been electrospun to produce aligned scaffolds for the study of neurite outgrowth and differentiation of neural stem cells seeded onto the scaffolds [117]. Yang et.al. also attempted to develop a porous polymeric nano-fibrous scaffold from PLLA for *in vitro* culture of nerve stem cells [118]. Other researchers utilized electrospun PLA scaffolds to investigate their morphology and biodegradation rates [119, 120].

Polyethylene glycol (PEG) is a water-soluble polymer with a wide range of molecular weights. PEG exhibits useful properties such as protein resistance, low toxicity and immunogenicity. Studies have shown that the PEGs can abrogate immunogenicity of proteins and can preserve their biological properties[121]. PEG is frequently chosen as drug carriers due to their biocompatibility, minimal toxicity and good solubility in water or other common solvents. PEG is also co-polymerized with linear aliphatic polyesters like poly(lactic acid) (PLA) to improve the biocompatibility of polymers for use in drug delivery systems and tissue engineering.

Poor hydrophilicity of PLA limits its use as scaffolds because it causes a low affinity for cells. An effective way to solve this problem could be the addition of biopolymers that are highly hydrophilic in general. In addition to the weak affinity of cell on PLA surface, hydrophobic character of PLA is also a general drawback in biomedical applications due to strong nonspecific adsorption of proteins onto its surface. This adsorption process triggers various undesired reactions in the body and leads to quick clearance of drug-loaded nano- and micro-particles from circulation. Surface hydrophilizations by chemical or physical procedures, including surface chemical reactions, plasma treatment and adsorption, are utilized to improve polarity and hence biocompatibility of hydrophobic polymer surfaces. PLA has been copolymerized with many polymers like PGA and PCL [122, 123]. PEG has been proved to be an efficient surface modifier to render polymer surface less hydrophobic, therefore to suppress nonspecific protein adsorption and detrimental bioadhesion[124, 125].

Zhao et.al. synthesized PEG-b-PLLA diblock copolymers with different molecular masses and compositions by ring-opening polymerization of L-lactide (LLA) with Sn $(Oct)_2$ as the catalyst and methoxy poly(ethylene glycol) (mPEG) as the initiator. The results showed that relative molecular mass of PEG-PLLA could be controlled by adjusting feed ratio of mPEG to PLLA, and hydrophilicity of PEG-PLLA increased with the increase in amount and/or length of mPEG chain [121]. The crystallization behavior, melting behavior, and nonisothermal crystallization kinetics of PLLA-PEG diblock copolymers were investigated by Yang et. al. [126]. It was documented that crystal forms of PLLA and PEG blocks are α-phase and monoclinic crystal. Moreover, melting behaviors of PEG homopolymer and PEG block of PLLA-PEG diblock copolymers are

very different. Xu et.al.[127] prepared emulsified Doxorubicin hydrochloride (Dox), a water-soluble anticancer agent, in chloroform solutions of PEG–PLA, which was then electrospun to form nanofibers with a sheath/core structure. In this structure, polymer constitutes the sheath while drug was entrapped in the core. Result showed that the release rate of Dox decreased as Dox content in the fibers increased. Moreover, Dox release consisted of three sequential stages that were all diffusion-controlled. Kim et. al. successfully incorporated a hydrophilic antibiotic drug, cefoxitin sodium, into electrospun PEG–PLA nanofibers. It showed that PEG–PLA block polymer could reduce accumulative amount of drug released at earlier time points and prolong drug release [2].

2.4 Drug Release From Electrospun nanofibers

Electrospun nanofibers are promising in targeted delivery and controlled release of drugs. Controlled drug delivery system is used to improve therapeutic efficacy and safety of drugs by delivering them to the site of action at a rate dictated by need of physiological environment. Large surface area to volume ratio of electrospun nanofibers allows increased exposure of molecules to nanofibers, creating more opportunities for binding and catalytic reactions. Drug molecules in polymer nanofibers can be present in three forms: the first even dissolution in nanofiber; the second formation of particles with nanofiber; and/or the third embed as a core encapsulated by a sheath polymer. Drug release kinetics in all three forms are based on morphology and porosity of nanofibers and the interactions between drug and matrix. In the first form, drug can be released into surrounding tissues by diffusion and it is driven by a concentration gradient. This is the most typical drug release when drugs are uniformly dissolved in the nanofibers. In the

second case where drug particles are located in nanofibers, slow biodegradation of the surface layers of nanofibers leads to the release of suspended drug. This release mechanism can be associated with a burst phenomenon [128]. However, the burst release of drugs can be prevented by the design of nanofiber with a sheath/core structure. The sheath/core structure protects the embedded drug (core) by enclosing drug in the polymer matrix (sheath). There are two possible structures for core composition: one is that the pure drug in either solid or liquid form constitutes of the core surrounded by a pure continuous polymer sheath; the other is that the drug molecules are dispersed in a polymer matrix and the whole dispersion system serves as the core [129, 130]. Anticancer drugs like doxorubicin hydrochloride (DOX) [127] and Paclitaxel (PTX) [3] have been incorporated inside electrospun biodegradable nanofibers by forming the first kind of core-sheath structure in which the pure drug constitutes of the core. PEG–PLA nanofibers with different Dox loadings were obtained by emulsion-electrospinning, in which a water solution containing Dox was emulsified in chloroform solution of PEG-PLA to obtain a stable water/oil emulsion before being electrospun into nanofibers [127]. PEO-FITC was incorporated into copolymer PEG-PLA, forming the second kind of core-sheath structure [131]. Antibiotics were also incorporated into electrospun nanofibers. Cefazolin, a broad-spectrum antibiotic, has been incorporated into poly(lactide-co-glycolide) (PLGA) electrospun nanofibers [132]. Another hydrophilic antibiotic drug (Mefoxin(R), cefoxitin sodium) was incorporated into electrospun poly(lactide-co-glycolide) (PLGA)-based nanofibrous scaffolds. It’s drug release behavior from the electrospun scaffolds and antimicrobial effects on Staphylococcus aureus were also investigated[133].

2.5 Surface Functionalization and Immobilization of Bioactive molecules

Extensive research has been performed to provide biopolymers with various functional groups that can be conjugated with specific bioactive molecules. Kim and Park [7]fabricated a biodegradable nanofibrous mesh of PCL and PLGA-*b*-PEG-NH_2 diblock copolymer with its fiber surface functionalized with primary amine groups. A model enzymes, lysozyme, was then covalently immobilized onto the surface of nanofibrous mesh using amine-reactive coupling agents. The amount of active amine group on the surface of nanofibrous mesh was found to be related to the amount of enzyme being immobilized. Patel et.al.[6] fabricated heparin-functionalized PLLA nanofibers by using di-NH_2-PEG as linker. Then an ECM protein [134] and basic fibroblast growth factor (bFGF) with heparin-binding domains were attached to the functionalized PLLA nanofibers. Results showed that the laminin modified nanofibrous mesh was able to induce neurite outgrowth and the immobilization of proteins, and that growth factors were able to promote cell migration [6, 134]. Ma and Ramakrishna [135] oxidized a regenerated cellulose [136] nanofibrous mesh with $NaIO_4$ to generate aldehyde groups, upon which proteins A/G containing six immunoglobulin G (IgG) binding domains was covalently immobilized.

Choi and Yoo [137] treated PCL-PEG/PCL block copolymers with fluorescein amine in acetone, and then conjugated the BSA labeled by fluorescein-5-isothiocyanate (FITC) to the amine groups on the surface of PCL-PEG/PCL block copolymers via its carboxylic groups. The ratio of PCL-PEG/PCL block copolymers was a factor to determine the active amine groups on the nanofibers' surface. The fluorescent proteins then showed an attenuated release profile. Jia et.al. [138] treated PCL nanofibrous mats with

radiofrequency generated Ar plasma, then immersed them in the SEP solution (soluble eggshell membrane protein). After 24-hour incubation, eggshell protein was successfully immobilized onto PCL nanofibers. SEM pictures showed that the surface of SEP-grafted fibers became rough and thick because of SEP grafting. Casper *et. al.* [139] coated electrospun collagen nanofibers with perlecan domain I (PlnDI) before having fibroblast growth factor 2 (FGF-2) bound to heparan sulfate chains on PlnDI. Immobilization of FGF-2 onto collagen nanofibers was found more effective in promoting cell proliferation than immobilized BSA. Other researches indicated that changes in the ratio of block copolymers would lead to changes in hydrophobicity, physical behaviors, degradation and biocompatibility of nanofibrous meshes [124, 140]

There has been several studies to modify polymer surface so as to enhance or reduce their capacity of immobilizing bioactive molecules by physical adsorption. Huang *et. al.* [141] showed that phospholipids modification would enhance poly[acrylonitrile-co-(2-methacryloyloxyethyl phosphorylcholine)]s (PANCMPCs) nanofibers' efficiency to immobilize lipase. In another study, PEG-b-PDLLA fibers were surface functionalized with biocytin or RGD peptide. The functionalized nanofibers were resistant to nonspecific adsorption of proteins and would therefore provide a "clean" surface for the interactions between cells and nanofiber[142].

Nanofibrous materials have been considered candidate scaffolds for cell adhesion and cell viability because of their morphological similarity to natural extracellular matrix[143]. When nanofibers produced by jet-blowing of PTFE 601A were coated onto glass surfaces, it was shown that hydrophobicity and large surface area of PTFE would provide better adsorption of BSA (bovine serum albumin). The inflammatory cytokines

expressed by macrophages cultured on PTFE showed that PTFE nanofibers were unable to give a significant inflammation response. Kim *et. al*. [144] demonstrated that egg shell protein modified PCL nanofibers might be a good scaffolds for dermal fibroblasts to grow because of its mechanical and hydrophilic characteristics. Researches concentrating on nerve cell adhesion and outgrowth on nanofiber scaffolds have been conducted [136, 145], and so have researches in introducing biomodified electrospun nanofibers for the purpose of repairing injured or damaged nervous system. Meiners *et. al*. [146] used neuroregulatory molecule, tenascin-C, to modify the surface of polyamide nanofiber scaffolds to improve spinal cord regeneration. Block copolymer (PEG-b-PCL) was also used in tissue engineering to bind specific cells like human dermal fibroblasts, with a cell adhesive peptide being attached to its PEG segment [147]. These successful *in vitro* and *in vivo* studies suggested possibilities of functional nanofibers' applications in neural regeneration. Researches also showed that plasma treated PCL nanofibrous scaffolds were superior to PCL/collagen scaffolds in enhancing the Schwann cell adhesion [148]. Nanofibrous scaffolds have been found valuable for their promising biodegradation properties, as well as excellent cell adhesion and proliferation [149, 150].

2.6. Summary

Electrospinning can produce nanofibers with large surface-volume ratio, good mechanical strength and porous structure. The fiber morphology and diameter can be controlled by changing electropinning parameters like applied voltage, tip-collector distance, concentration of polymer solution, etc. Nanofibers can be electrospun from both synthetic polymers such as PLA, PCL and natural polymers such as chitosan and collagen. Bioactive molecules, such as drugs and/or proteins, can be incorporated into the

nanofibers to provide functional nanofibers that are useful for biomedical applications. Surface property of nanofibers can be changed to make them more hydrophilic for cell attachment and proliferation.

The present study is to develop multi-functional nanofibers that are incorporated with antibiotics and immobilized with model proteins on the surface. Specifically, a model antibiotic, Tetracycline hydrochloride (TCH) was loaded into PLLA/PLLA-b-PEG nanofibrous mat via emulsion electrospinning. The drug-loaded nanofibers were then surface-modified to allow a model protein, Bovine Serum Albumin (BSA) to be covalently immobilized onto the nanofiber's surface. BSA labeled with two different fluorescence dyes were immobilized onto the nanofiber surface respectively via two different functional groups on fiber surface. These nanofibers are potentially useful for wound healing and tissue engineering scaffolding and can provide both infection control and promotion of wound healing or tissue regenerations.

Chapter 3 Materials and Methods

This chapter will introduce the materials and equipments used for this study and delineate the procedures of all the related experiments, including emulsion electrospinning for the incorporation of a drug into nanofibers, contact-angle test for the evaluation of surface properties of nanofibers, surface functionalization of drug-loaded nanofibers, immobilization of proteins, monitoring drug release profiles, and antibacterial tests for thedrug-loaded nanofibers.

3.1 Materials

The following chemicals were purchased from Sigma Aldrich Canada: Benzyltriethylammonium Chloride (98%), 2-Mercaptoethanol, Bovine Serum Albumin (96%), Albumin FluoresceinIsothiocyanate Conjugate Bovine, and Tetracycline hydrochloride (TCH, ≥95% purity).

The following chemicals and supplies were purchased from Thermo Fisher Scientific Canada: NaOH (≥98%), 1-ethyl-3-(3-dimethyl aminopropyl) carbodiimide hydrochloride (EDC),sulfo-N-hydroxysuccinimide (NHS),Ethylene Glycol-bis (Succinimidylsuccinate) (EGS), BBL^{TM} Mueller Hinton II Agar, and Snake Skin Pleated dialysis tubing (cut-off MW=7000).

L-lactideand PLLA (MW 220×10^3 g/mol) was supplied by Purac.

HO-PEG-NH_2 was purchased from JenKem Technology USA Inc. (Allen, TX, US) for the preparation of PLLA-b-PEG-NH_2. For that purpose, HO-PEG-NH_2 was dissolved in a mixture of aqueous NaOH and THF(tetrahydrofuran), and Di-tert-butyl dicarbonate (Boc_2O) was added so as to yield HO-PEG-^{N}Boc. The diblock copolymer PLLA-b-PEG-

^{N}Boc was prepared with ring opening polymerization of L-lactide in the presence of HO-PEG-^{N}Boc as macroinitiator and ZnEt2 as catalyst. PLLA-b-PEG-^{N}Boc was then dissolved in a mixture solvent of CH_2Cl_2 and trifluoroacetic acid (TFA) at 0 °C for 2 h. TFA and CH_2Cl_2 was removed in vacuum, and the remaining solid was dissolved in a mixture of choloroform and triethylamine. PLLA-b-PEG-NH_2 was then precipitated out as the final product. The number average molecular weight of the block copolymer had been found to be 10,000 kDa by GPC (gel permeation chromatography), and its polydispersity is 1.3, indicating a narrow molecular weight distribution. And the NMR (nuclear magnetic resonance) spectrum is showing in Figure 3.1.

Figure 3.1 NMR spectrum of the block copolymer PLLA-b-PEG-NH_2

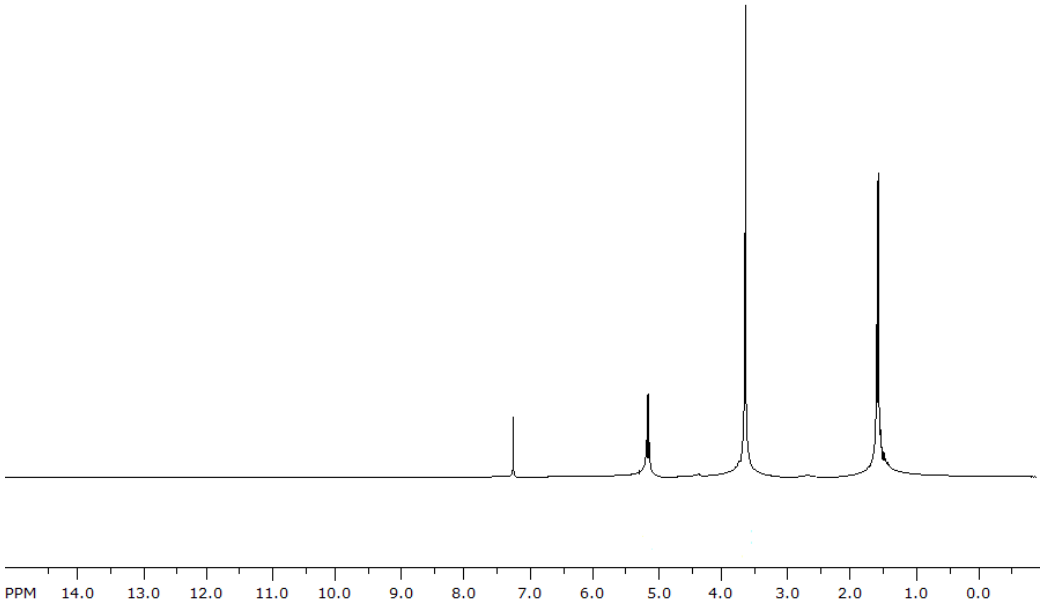

3.2 Fabrication of nanofibers by electrospinning

Shown in Figure 2.1 is the electrospinning apparatus for the fabrication of PLLA nanofibrous mat. For such fabrication, PLLA was dissolved in the solvent of chloroform at a concentration of 7.5% (w/w) and benzyltriethylammonium Chloride (BTAC) was added into the electrospinning solution as a surfactant (5% of the weight of PLLA) to lower the surface tension of the spinning solution. The polymer solution was kept overnight and magnetic stirred to completely dissolve the PLLA. For electrospinning, the polymer solution was added into a 5ml syringe with a stainless steel needle (18 gauge, blunt end),and then delivered to the needle by a PHD 22/2000 infusion syringe pump (Harvard Apparatus Canada) at a constant feed rate of 7ml/h. The stainless steel needle was connected to an ES 30 high voltage DC power supplier (Gamma High Voltage Research, Ormond Beach, FL). The electrospinning was performed in an ambient temperature and at the voltage of 22 kV. The distance between tip of the needle and ground collector was 20cm.

Nanofibers as a blend of PLLA-PEG-NH_2 and PLLA were prepared in a similar way as described above. Namely, benzyltriethylammonium Chloride (BTAC) was added into the electrospinning solution as a surfactant (5% of the weight of the polymers) to lower the surface tension of the polymer solution. PLLA/ PLLA-PEG-NH_2 at the blend ratio of 70:30 was electrospun at a fixed concentration of 7.5% (w/w) in room temperature, at the voltage of 22 kV, and at the 7ml/h flow rate, with a distance of 20cm between tip of the needle and the collector. Since the copolymer synthesized in our lab has a relatively low molecular weight (10×10^3 g/mol) for direct electrospinning, the blend mixture of PLLA

and copolymer was used in this experiment. Randomly oriented nanofibers were collected on a ground collector and also on silicon wafers for morphology examination under a Scanning Electron Microscopy (SEM, Cambridge Stereoscan 120).

3.3 Fabrication of Tetracycline hydrochloride loaded nanofibrous mat by emulsion elctrospinning

Emulsion electrospinning was used in this study to incorporate a hydrophilic drug into hydrophobic polymer nanofibers [8, 151]. Usually, an electrospinning process deals with a homogeneous solution in which all components (the polymer and the drug) are dissolved in the same solvent. In the emulsion electrospinning, the first step was to prepare an aqueous solution of drug (water phase) that would be emulsified into a polymer solution (oil phase), and then the w/o emulsion was electrospun. A core sheath structure was formed during emulsion electrospinning. According to Xiuling Xu et al [131], the emulsion droplet moves from surface towards the center during the stretching and evaporation of the solvent. Since chloroform is more volatile than water and evaporates much faster, the viscosity of polymer matrix increases much more quickly than the drug solution. This viscosity difference between the polymer matrix and the drug solution results in an inward movement of the drug towards the fiber axis, and eventually forms the core-sheath structure. This phenomenon is called “stretching and evaporation induced de-emulsification”. In the core-sheath structure, the drug is incorporated inside of the nanofibers instead of depositing on the fiber surface, and thus will not quickly release upon contacting with the releasing media, so that the so-called burst-release may be avoided. Another potential advantage of emulsion electrospinning is that different

solvents can be used for different drugs and polymers, so that there is no need for a common solvent. As a result, various combinations of hydrophilic drugs and hydrophobic polymers can be employed.

1 ml water solutions containing 3wt% or 6wt% of TCH (with respect to the weight of PLA-PEG-NH_2) was emulsified in 20 ml polymer solution of 7.5%(w/w) PLLA/PLLA-PEG-NH_2dissolved in chloroform. The emulsification was performed using a homogenizer (Silverson Mixer) at approximately 7000 rpm for 20 minutes. Throughout the process of emulsification, the emulsion was kept in an ice bath to avoid chloroform evaporation by heat generated from the homogenizer. In order to obtain stable and homogeneous W/O emulsions, 5%(w/w)of BTAC (with respect to the weight of PLLA/PLLA-PEG-NH_2) was added to the oily phase prior to emulsification as a surfactant to lower the surface tension of the polymer solution. After homogenizing for 20 minutes, the aqueous droplets were dispersed into the oily phase, forming a homogeneous W/O emulsion. The emulsion electrospinning process was then repeated under similar conditions. The same method was also used for the preparation of TCH loaded PLLA nanofibers.

To visualize the distribution of drug(s) in the emulsion electrospun nanofibers, 1wt% Fluorescein (with respect to the weight of polymer) loaded PLLA and PLLA/PLLA-PEG-NH_2hybrid nanofibers were prepared using the same emulsion electrospinning method described above.

3.4 Surface functionalization of electrospun nanofibers and immobilization of BSA

BSA was used as a model protein in this work to develop functional nanofibers. Figure 3 demonstrates the procedures to immobilize two BSAs (FITC-BSA and Rhodamine-BSA, respectively) onto the drug-loaded nanofibers.

Figure 3.2 Surface functionalization procedures for PLLA/PLLA-PEG-NH_2 nanofibers.

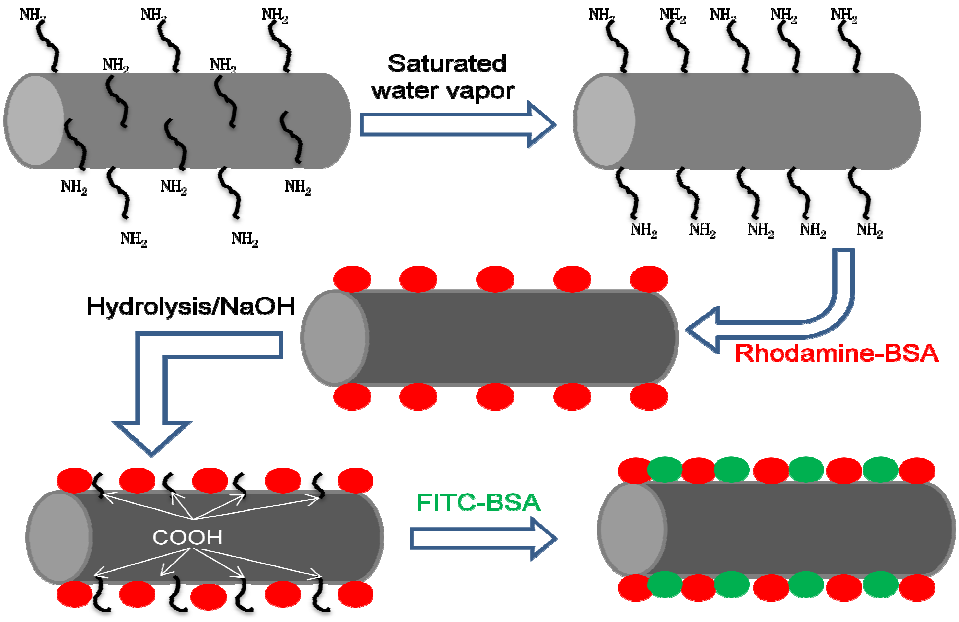

3.4.1 Exposure of amine groups and carboxylic groups on a fiber surface

For BSA immobilization, the electrospun hybrid PLLA/PLLA-PEG-NH_2 mat was pretreated with saturated water vapor at room temperature for 15min to allow a full exposure of amine groups to the mat surface so as to enhance the efficiency of BSA immobilization.

Density of reactive carboxylic groups on PLLA and hybrid nanofibers was found to increase when a nanofibrous mat was treated in 0.01M NaOH solution or 0.01HCl solution for different periods of time at 37^0C[6]. The electrospun nanofibrous mats were treated in alkaline or acid for 15, 30 and 60 minutes. Their hydrophilicity were then tested using a contact angle goniometer (Rame-hart, Inc.)so as to find out the most efficient conditions for future surface functionalization.

3.4.2 Contact angle tests

Figure 3.3 Contact angle goniometer (ramé-hartModel 200)

The angle between the solid surface and the liquid/vapor interface is referred to as the contact angle. It can be determined by referring to interactions across the three interfaces: solid-liquid, solid-vapor and liquid-vapor [152]. The term “wetting” is used to describe contact between the liquid and solid surface, which is the result of the intermolecular

interaction between the two surfaces. The “wettability” or “hydrophilicity” of the solid surface is a function of the energy (i.e. surface tension) of the interfaces involved, and the degree of hydrophilicity is described by the contact angle. For a flat solid surface, it’s contact angle is measured by a suitable liquid resting on the solid surface. As shown in Figure 3.4, if the solid surface is strongly hydrophilic, the droplet of the liquid will quickly spread out on the solid surface, and the contact angle will be close to zero. When the solid surface is less hydrophilic, the contact angle will be up to 90°. If the surface is hydrophobic, the contact angle will be larger than 90°. When the contact angle exceeds 150°, the solid surface is called a surperhydrophobic surface [153-155].

Figure 3.4 Degree of different levels of surface hydrophilicity[155]

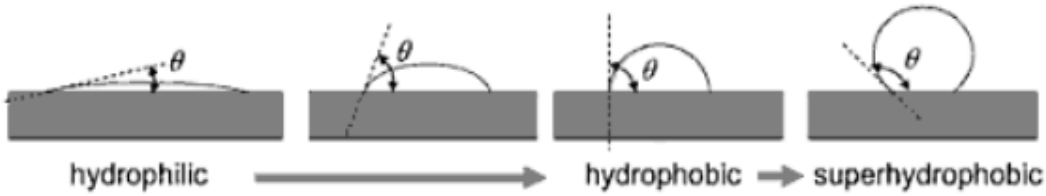

Contact angle was used in our project to determine the hydrophilicity of electrospun nanofibrous mats that had been treated with alkaline or acid for 15, 30 and 60 minutes. When the PLLA and hybrid PLLA/PLLA-PEG-NH_2nanofibrous mats were treated with alkaline or acid, they would be subjected to the process of surface hydrolysis so as to have two hydrophilic chemical groups (carboxylic groups and hydroxyl groups) exposed onto the surface and,as a result, to have the mats’ surface hydrophilicity much improved. The contact angle goniometer(Figure 3.3) and a DROPimage were used to measure the contact angle according to the manual [156].

Figure 3.5 Scheme of the contact angle goniometer

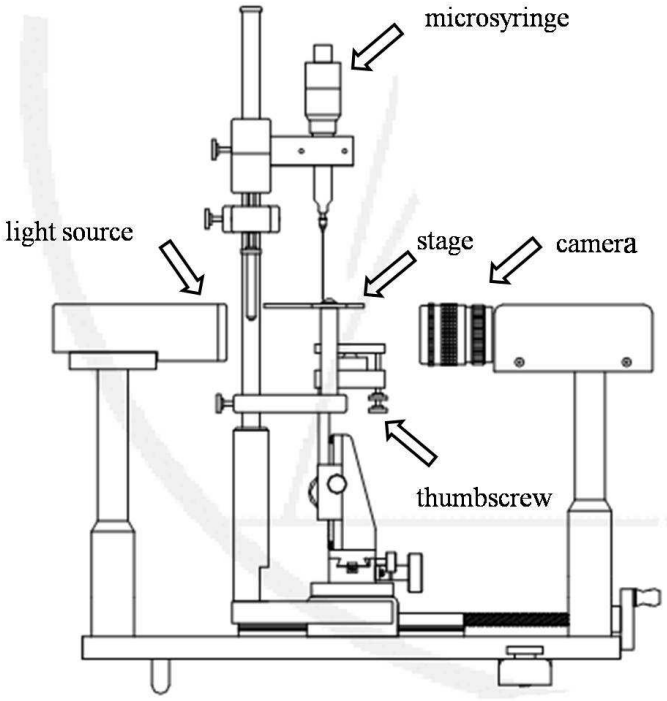

As shown in Figure 3.5, the procedures of the test can be briefly described as follows:

1. Set up the goniometer and DROPimage program and have them ready for use: tune on the light source and have the camera ready for use, use the thumbscrew to adjust the stage until the tilt value shown in the image window is 0.

2. Adjust position of the microsyringe and move the needle to the center of the window screen, raise the stage to about just below the midpoint of window screen and get ready to create a water drop, lower the microsyringe and use the horizontal increments on the microsyringe to determine volume of the drop and, when the drop

reaches the stage, slowly raise the needle so that it will release and create a drop on the stage.

3. Use the DROPimage program to measure the contact angle: set the position of the vertical and horizontal lines in the program window so that the vertical line passes through the center of the drop and the horizontal line is alongside the baseline, click the measure button and the contact angle measurement results get recorded.

3.4.3 Immobilizing the first layer of BSA onto the PLLA-PEG-NH_2

Figure 3.6 Reaction for immobilizing the BSA onto the copolymer

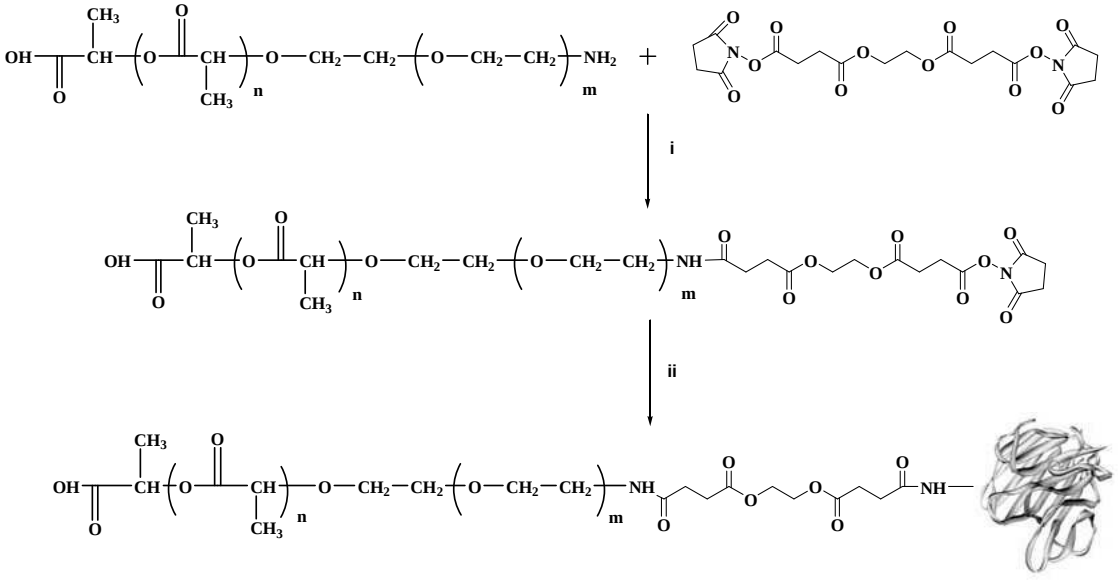

represents the BSA molecule, i) having agitated for 1h at room temperate; ii) having reacted with BSA for 30min

Before reacting with EGS, the amine groups on the hybrid mat were exposed to saturated water vapor for 15min. Each electrospun hybrid PLLA/ PLLA-PEG-NH_2nanofibrous mat(5mg) was then immersed in 20ml DMSO containing 60μmol Ethylene Glycol-bis (Succinimidylsuccinate) (EGS) and gently agitated for 1h at room temperature. After being rinsed with distilled water for three times, the activated sample was immersed in 20ml PBS containing 4.5mg BSA for 30min so that the BSA molecules could be covalently attached to the primary amine groups on PLLA-PEG-NH_2.

3.4.4 Immobilizing the second layer of BSA onto PLLA-PEG-NH_2 and one layer of BSA onto PLLA

Figure 3.7 Reaction for immobilizing the BSA onto the PLLA

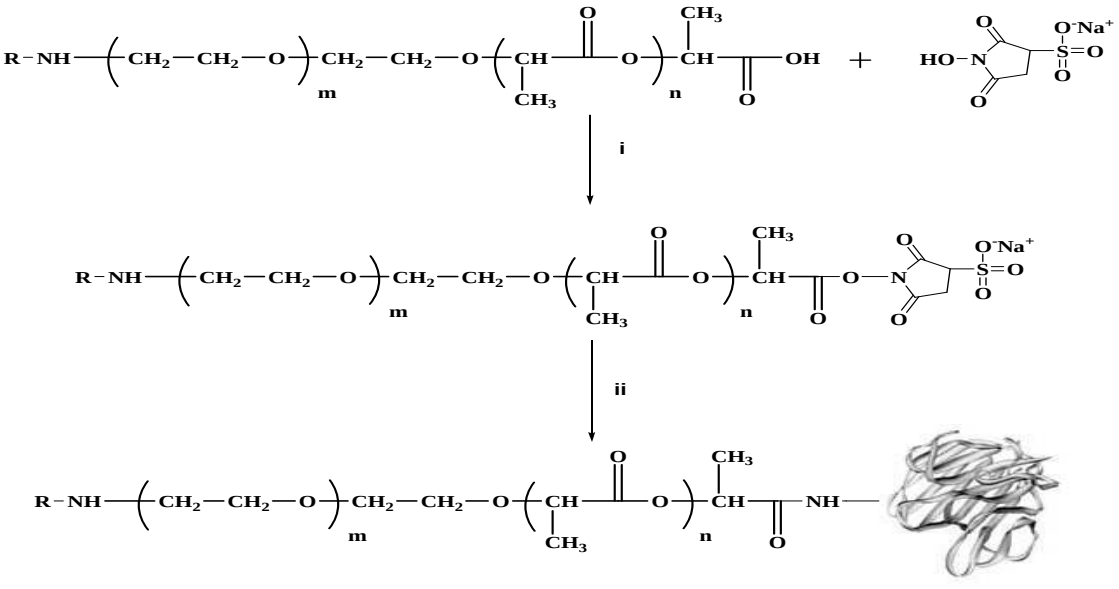

 represents a BSA molecule, R represents H or BSA: i) having reacted in the presence of EDC at room temperature for 15min and been quenched with mercaptoethanol, ii) having reacted with BSA for 2h

The carboxylic groups on PLLA may be reacted to NHS in the presence of a carbodiimide like EDC, resulting in a semi-stable NHS ester, which may then be reacted with the primary amine groups on BSA to form amide crosslinks. Such a process is expected to enhance the efficiency of coupling.

Before conjugating protein onto the PLLA and PLLA/ PLLA-PEG-NH2 hybrid nanofibrous mats, the mats were first treated with 0.01M NaOH solution for 15min to expose the carboxylic groups of PLLA on the mats' surface, which will then be allowed to react with sulfo-NHS to produce NHS ester so as to make the reaction much easier between carboxylic groups on the surface and BSA molecules.

The PLLA and hybrid mats were then rinsed with distilled water, immersed in 20ml PBS containing 8mg EDC and 22mg sulfo-NHS, shaken gently and allowed to react at room temperature for 15min. After the reaction, 28μl mercaptoethanol was added to the solution and adequately shaken to quench the residual EDC. 3ml of 1.5mg/ml BSA was then added to the solution and incubated for 2 hours at room temperature to allow the BSA covalently attached to the carboxylic groups of PLLA.

3.4.5 Preparation of Confocal samples

In order to confirm that the BSA had successfully been immobilized on the fiber surface, fluorescent conjugated BSA was immobilized onto the nanofibers to allow direct observations under a Confocal laser scanning microscopy (CLSM, Olympus IX-70).

Rhodamine-BSA was prepared by dissolving rhodamineisothiocyanate in DMSO at a concentration of 5mg/ml. In a dark lab, 50μl of rhodamine solution was slowly added to each ml of BSA solution (1.5mg/ml).The mixed solution was gently stirred and incubated over night at room temperature, transferred into a MW7000 cut-off dialysis bag, and then dialyzed overnight in a PBS solution (pH7.4) to remove the residual rhodamine. Rhodamine-BSA was obtained as a result.

PLLA and hybrid nanofibers collected on slides were then allowed to react with FITC-BSA (Sigma) and Rhodamine-BSA, in the same way as described in 3.4.3 and 3.4.4.

3.4.6 ATR-FTIR examination of protein's secondary structure

FTIR is an established technique for the analysis of the secondary structure of proteins. ATR-FTIR (NICOLET iS10, Thermo Scientific) was used in our study to confirm immobilized proteins on the surface of nanofibrous mats. Each mat was put on a crystal and given a proper pressure to stabilize the sample. The crystal material used in the experiment was diamond.

3.4.7 Quantification of immobilized BSA

In order to determine the amount of BSA immobilized on the PLLA and hybrid PLLA/PLLA-PEG-NH_2nanofibrous mats, the procedures described in 3.3.3 and 3.3.4 were repeated in dialysis bags (cut-off MW=7000). After reacting with EGS and immobilizing the first layer of BSA, the mat was taken out and washed three times. After the reaction, remainder of the solution was transferred to a dialysis bag(dialysis bag A). The mat was then allowed to react with EDC and sulfo-NHS in another dialysis bag(dialysis bag B) as described in 3.3.4, and was again taken out and washed with distilled water for three times. After immobilizing the second layer of BSA, remainder of the solution was transferred to a third dialysis bag (dialysis bag C). The two dialysis bags (A and C) holding the leftover solution were allowed to undergo dialysis overnight in PBS7.4 solution to remove the residual small molecules other than BSA. The two solutions were then collected and their absorption checked at 275nm under a UV-vis spectrometer. BSA standard curve was plot as the UV absorption at the various BSA concentrations of 10, 5, 2.5, 1.25, 1, 0.5, and 0.25μg/ml, resulting in the revelation that the BSA concentration is a linear function of its UV absorption. The amount of BSA left in the solution was then determined by comparing it to the BSA standard curve, and the amount of BSA immobilized was calculated by deducting the amount of BSA left in the solution from the total amount of BSA added.

3.5 In-vitro drug release

The release of TCH from the electrospun nanofibers loaded with drug was detected by a UV-vis spectrometer at the wavelength of 366nm. Each TCH loaded nanofibrous mat (5mg) was placed in the dialysis bag (cut-off MW=7000) incubated in 30ml PBS(pH=7.4,

0.01M) at a 37^0C water bath and gently shaked. At predeterminated time intervals (every 24 hours), 6ml of the incubation solution was taken out and 6ml fresh PBS (pH7.4) was added into the solution. The sample solution taken out was then tested to quantify the TCH according to its standard curve. The TCH standard curve was plot as the UV absorption at the various TCH concentrations of 20, 15, 10, 5, 1, 2.5, 1.25μg/ml, and the TCH concentration was found to be a linear function of the UV absorption. The accumulated release of TCH was then calculated as a function of the incubation time.

3.6 The microbial susceptibility test

3.6.1 Preparation of agar plates

The following items were autoclaved accordingly: test tubes and test tube rack, pipette tips, tweezers wrapped with aluminum foil, label tapes, cylinders, beakers, one bag of cotton-tip applicators, and one bottle of distilled (DI) water (1L) (autoclaved according to liquid autoclaving settings). A disinfection tape was put on what was to be disinfected.

Thirty eight grams of the Mueller Hinton II agar powder was dissolved in 1L of purified water. They were mixed thoroughly with heating and frequent agitation, boiled for 1minute until the powder was completely dissolved, and autoclaved at 121^0C for 30 min. The autoclaved agar solution was kept in a biosafety cabinet, and poured onto sterile polystyrene petri dishes quickly before the solution solidified. The amount of agar solution in each dish was such that it reached to about 1/3 of the height of the dish. The agar was then allowed to cool down and solidify in the biosafety cabinet.

The cryogenic vial filled with storage beads was removed from a -80℃ freezer. One bead was opened that removed using a sterile applicator. The bead was rubbed over the media with an applicator. The bead and the applicator were then disposed into garbage bin lined with a plain clear autoclave bag with biohazard logo tape for identification. The media was then kept in a 37℃ incubator for24 hours.

3.6.2 Plate inoculation

In the biosafety cabinet, 3 ml of distilled, deionized water was transferred into a test tube. 2-3 colonies were picked up with a cotton-tip applicator and dispersed into the water and vortex completely to make a bacterial suspension. Under the lamp, turbidity of the bacterial suspension was compared with that of the 0.5 McFarland standard. When it was found less opaque, more colonies would be picked and dispersed into the same suspension until it was of a turbidity similar to that of the standard. The suspension was then diluted to get the10^5, 10^4, 10^3, 10^2, 10^1, and 10^0 colony forming units (CFU)/ml.

After a 15 min adjustment of the turbidity, a sterile cotton swab was dipped into each of the inoculum and rotated against the wall of the tube above the liquid to remove the excess inoculum. The surface of each agar plate was streaked three times with each inoculum of a certain colony amount, the plate being rotated approximately 60° between the streakings to ensure even distribution. Touching the wall of a petri plate should be avoided as it may create aerosols. The inoculated agar plates were kept in the 37℃ incubator and, 24 hours after, number of the colonies was counted. The number of colonies on the agar plates should be on the decrease, and the area inoculated with the 10^1unit should have around 10 colonies whereas the area inoculated with the 10^0 unit

should have 0-1 colony. This procedure was used to confirm the accurate adjustment of the turbidity.

As shown in Figure 3.9, the number of colonies would decrease with decreased suspension concentration, and the number of colonies in the area inoculated with 10^2, 10^1 and 10^0 units were within the acceptable range. Thus it was confirmed that the turbidity adjustment was accurate.

Figure 3.8 Adjustment of inoculums turbidity

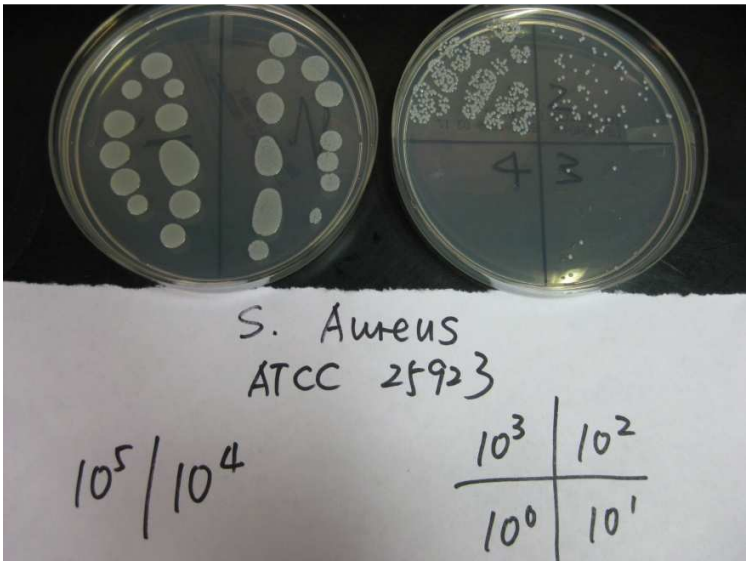

3.6.3 Sample Application

A disk (0.6 cm in diameter) cut from P3-1(a 3 wt% TCH-loaded PLLA nanofibrous mat), P3-2(a 3 wt% TCH-loaded BSA containing PLLA nanofibrous mat, BSA conjugated once), and H3-3(3 wt% TCH-loaded BSA containing hybrid nanofibrous mat, BSA conjugated twice), respectively, was tested. Positive control was made by dropping

3 wt% TCH (with respect to the average disk weight) onto a blank disk of nanofibrous mat. And a blank nanofibrous mat was used as a negative control. Sample disks with 6 wt% TCH were also prepared in manners described in the above. Specifications and abbreviated names of samples used for microorganism susceptibility test were listed in Table 3.1.

Table 3.1 Sample names and specifications

	PLLA nanofiberous mat	PLLA nanofiberous mat conjugated with BSA	Hybrid (PLLA/PLA-b-PEG) nanofiberous mat	Hybrid nanofiberous mat conjugated with BSA	Hybrid nanofiberous mat immobilized with 2 layers of BSA
Blank	P0-1	P0-2	H0-1	H0-2	H0-3
3% TCH	P3-1	P3-2	H3-1	H3-2	H3-3
6% TCH	P6-1	P6-2	H6-1	H6-2	H6-3

A commercially available TCH-sensitive bacterium, *Staphylococcus aureus* ATCC 25923 (American Type Culture Collection, Seattle), was used for this test. After sterilizing the working bench with UV irradiation of, the disks to be tested were placed on the agar plates seeded with S. aureus (i.e. applied to the agar surface with a pair of sterile forceps). To ensure complete contact of the disk with the agar, gentle pressure was applied with the forceps. Caution was needed not to place the disks closer to each other than 24mm from center to center, and not to relocate a disk when it was in contact with the agar surface. The disks were then incubated in a CO_2 incubator at 37 ºC for 24 h. The

study of antibacterial activity of the tested disks against Staphylococcus aureus lasted for 7 consecutive days or until the samples had no antibacterial ability. 24 hours after, the inhibitory effect of each sample disk was evaluated by referring to the diameter of the clearing around a disk where bacteria had not been able to grow (the clearing known as the inhibition zone).Then the sample disks were transferred to fresh bacterial-streaked agar platesfor the examination of the inhibitory effect provided by the remainder of the drug in the disk. The plates were read only when the lawn of growth had become confluent or nearly confluent. Caution was such that transmitted light was used, and the plate was held between the eyes and source of the light, and that diameter of the inhibition zone was measured from the back of the plate, to the nearest millimeter. Diameter of the inhibition zone of each sample disk was then measured using a vernier caliper and averaged. The antibacterial experiments were performed in triplicate. All results were expressed as the mean± SD (standard deviation of the mean). Student t-test was used to determine the significant differences among the groups. A *P* value less than 0.05 was considered to be significant (Table 4.3).

Chapter 4 Results and Discussion

Presented and discussed in this chapter are results of the experiments, including SEM and Confocal images, drug release profiles, FTIR-ATR spectra and microorganism susceptibility tests for the functional nanofibers. Potential application of the developed nanofibers in biomedical fields will also be discussed.

4.1 Morphology of electrospun nanofibers under scanning electron microscopy (SEM) and laser scanning confocal microscope

It was found that the morphology of electrospun nanofibers could be affected by such processing parameters as field voltage, distance between needle tip and collector, solution concentration and viscosity, etc. It is known that the amount of beads and area density of nanofibers increases when the tip-collector distance increases, and decreases when there is an increase in the field voltage [72]. After several trials, the electropinning conditions that would provide the best quality of nanofibers were found to be: 22kv, 7ml/h flow rate and 12cm tip-to-collector distance. Under these conditions, nanofibers were collected on an aluminum foil as fiber mat. Different samples were cut from the nanofibrous mat for SEM examination. The fiber diameter and morphology were found to be different for samples into which different amounts of drug had been loaded, as shown in Table 4.1. The average diameter of PLLA nanofibers was larger than that of the hybrid PLLA-PEG-NH_2/PLLA nanofibers (blend ratio: 30:70). This was mainly due to the decreased viscosity of hybrid polymer solution as the copolymer PLLA-PEG-NH_2, owing to its lower viscosity, had a lower molecular weight. The copolymer was more hydrophilic than PLLA because of its PEG block, and a hydrophilic polymer was found to decrease the viscosity of electrospinning solution, thus decreasing the diameter of

nanofibers [7, 157]. After loading TCH into the nanofibers, the fiber diameter increased slightly by 100-200nm for the PLLA nanofibers. The larger amount of TCH loaded, the bigger the fiber diameter. The diameter of hybrid nanofibers also increased after loading drug into them, but significant difference was not found when different amounts of drug had been loaded. The standard deviations of drug-loaded nanofibers were found to be relatively large, which could be due to the instability of emulsions towards the end of the electrospinning processes. At the end of electrospinning processes, the TCH water solution (water phase) started to dissociate from the polymer solution (oil phase). This instability was even more severe in the electrospinning process of emulsion containing 6%TCH.

Table 4.1 Diameter(nm) for electrospun nanofibers with different amounts of drug loaded.

	Blank	3% TCH loading	6% TCH loading	BSA conjugated
PLLA	670±150	688±223	735±220	1506±460
Hybrid	579±109	650±148	657±203	1505±620

Figure 4.1 shows the SEM images of PLLA and hybrid nanofibers into which different amounts of TCH had been loaded. As shown in Figure 4.1A and D, the blank PLLA and PLLA-PEG-NH_2/PLLA hybrid nanofibers are uniform and smooth on the surface. The

nanofibers with drug loaded (Figure B, C, E, F) also appear to be smooth on the surface without any drug crystals, which indicates that the drug was successfully incorporated into the fibers. However, some fibers look much bigger than others or have expanded into some part of the fiber, while some fibers look very small. This indicates that TCH may aggregate in some part of the fiber to result in uneven fiber diameters.

Figure 4.2 shows the confocal images of fluorescein-loaded PLLA and hybrid nanofibers. Fluorescein was incorporated into the nanofibers by the same method as for TCH. The incorporated fluorescein shows green fluorescent throughout the entire fiber, and seems to be more evenly distributed in hybrid nanofibers than in plain PLLA nanofibers since the former contain more hydrophilic copolymers that will lead to a stabler water-in-oil emulsion. According to previous researches, there are mainly two polymeric delivery systems: matrix and reservoir structures[158, 159]. In the matrix structure, the drug is dispersed throughout the polymer matrix, and drug release rate is controlled by diffusion which decreases with time. In the reservoir structure, the drug is incorporated into the polymer matrix by the so-called “core-sheath” structure, in which the drug serves as the core and the polymer matrix as the sheath, hence the sustained and controlled release of the drug. As shown in Figure 4.2, the fluorescein incorporated into the PLLA gets distributed throughout the fiber, without forming the core-sheath structure. However, the fluorescein-loaded hybrid nanofibers (Figure 4.2 B) shows a much clearer and more desirable structure with the fluorescein acting as the core because the hybrid nanofibers has been electrospun from a more hydrophilic polymer solution, which has given a stabler emulsion to favor the distribution of water-soluble drugs.

Figure4.1 SEM micrograph of drug-loaded nanofibers

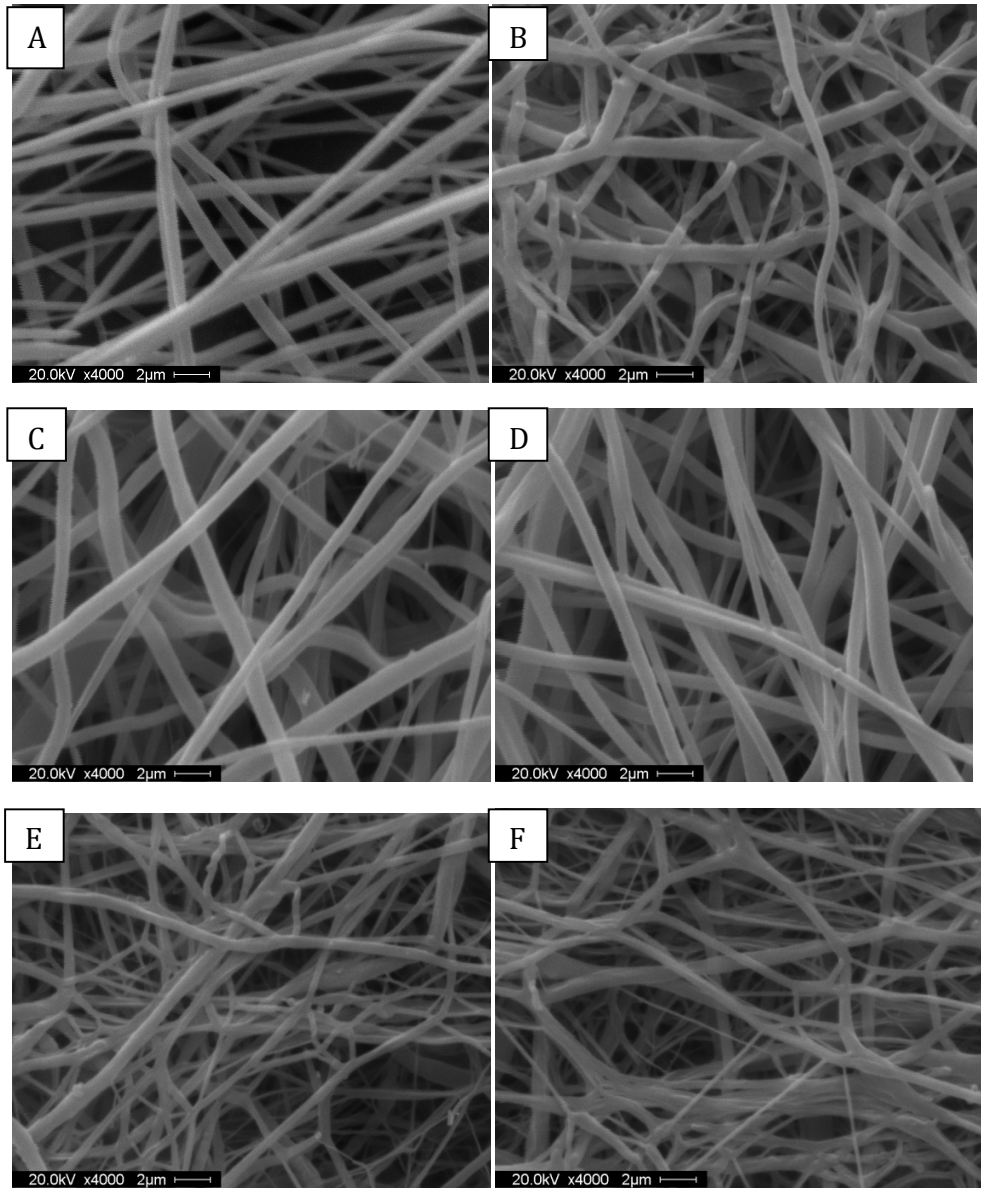

A:P0-1,B:P3-1, C: P6-1, D: H0-1, E:H3-1, F:H6-1

Figure 4.2 Confocal image of fluorescein-loaded nanofibers

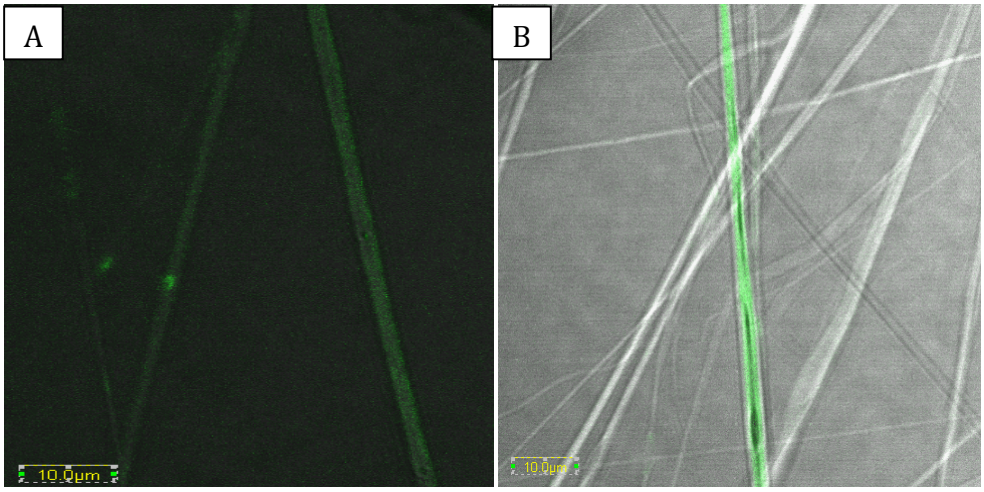

A: PLLA with fluorescein, B: hybrid with fluorescein

4.2 Surface hydrolysis and contact angle test

Surface hydrolysis was designed to turn hydroxyl groups on the surface of PLLA nanofibers into carboxylic groups, and was in order to prepare the PLLA nanofibrous mat for the further immobilization of protein. The degree of surface hydrolysis with HCl and NaOH was determined by the contact angle test. After surface hydrolysis, the contact angles of both HCl treated PLLA nanofibrous mat (Figure 4.3B) and NaOH treated mat (Figure 4.3C) were obviously smaller than that of the mat that had not undergo such treatment (Figure 4.3A). As discussed in Chapter 3.4.2, the degree of surface hydrophilicity is described by the contact angle, hence the more hydrophilic surface the smaller contact angle between surface and droplet (see Figure 3.4). Figure 4.3 thus indicates that treating the mat with HCl or NaOH will result in its improved surface hydrophilicity. As shown in Figure 4.4, contact angles will decrease after treating with

0.01M HCl for 15min, 30min and 1h. However, the PLLA nanofibrous mat has the smallest contact angle after HCl treatment for 15min. The contact angle also decrease dramatically after treating with 0.01M NaOH. As shown in Figure 4.4, the PLLA nanofibrous mat after treating with NaOH for 1h has the smallest contact angle, which also means the mat has the highest hydrophilicity. But since NaOH is a very strong alkali and highly corrosive, the PLLA nanofibrous mat could hardly maintain its morphology, but shrink into small pieces after treating with NaOH for 1h. This phenomenon has not been observed in HCl treated samples because an acid solution usually has a smaller capacity of hydrolysis than an alkali solution of the same concentration. When nanofibrous mats are treated for the same length of time, the PLLA nanofibrous mats treated with 0.01M NaOH will have a smaller contact angle than that treated with 0.01M HCl, suggesting that NaOH is more likely to provide a hydrolysis surface. In order to achieve the maximum hydrophilicity and yet maintain the integrity of PLLA mats, treatment of 0.01M NaOHfor 15min was chosen for all PLLA and hybrid mats in our subsequent work.

Figure 4.3 Contact angle test

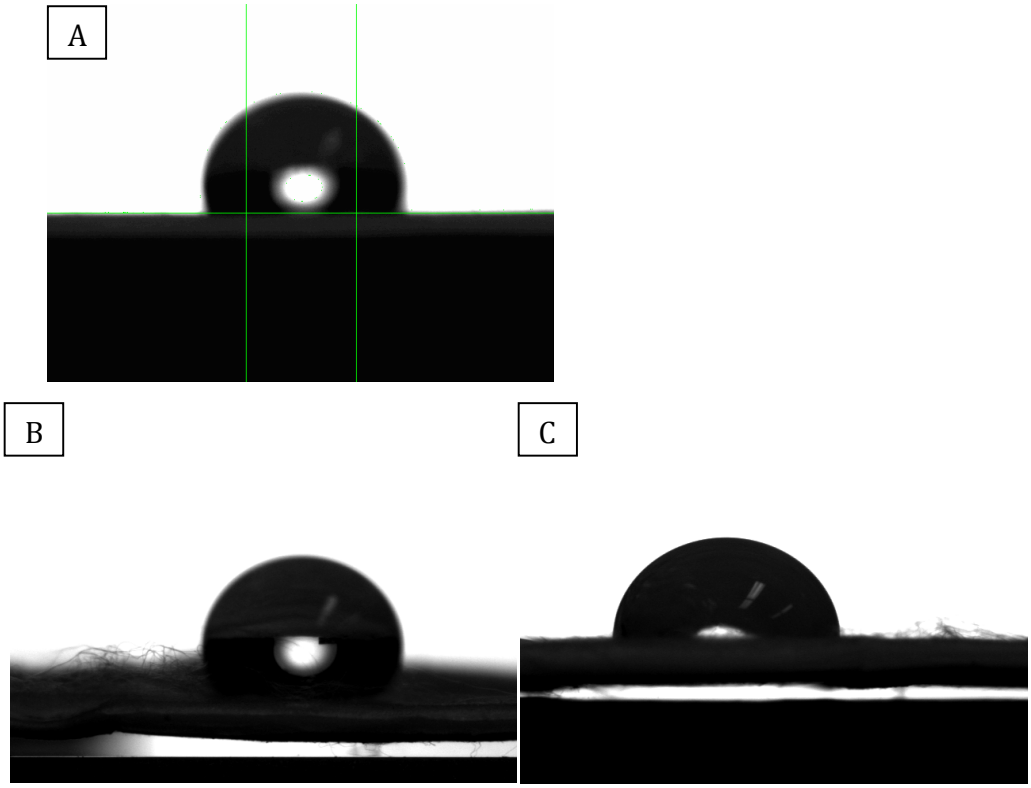

A: PLLA nanofibrous mat, B: 15min HCl treated PLLA nanofibrous mat, C: 15min NaOH treated PLLA nanofibrous mat

Figure 4.4Changes of the contact angle of PLLA nanofibrous mats after hydrolyzing with HCl and NaOH for 15min, 30min and 1h

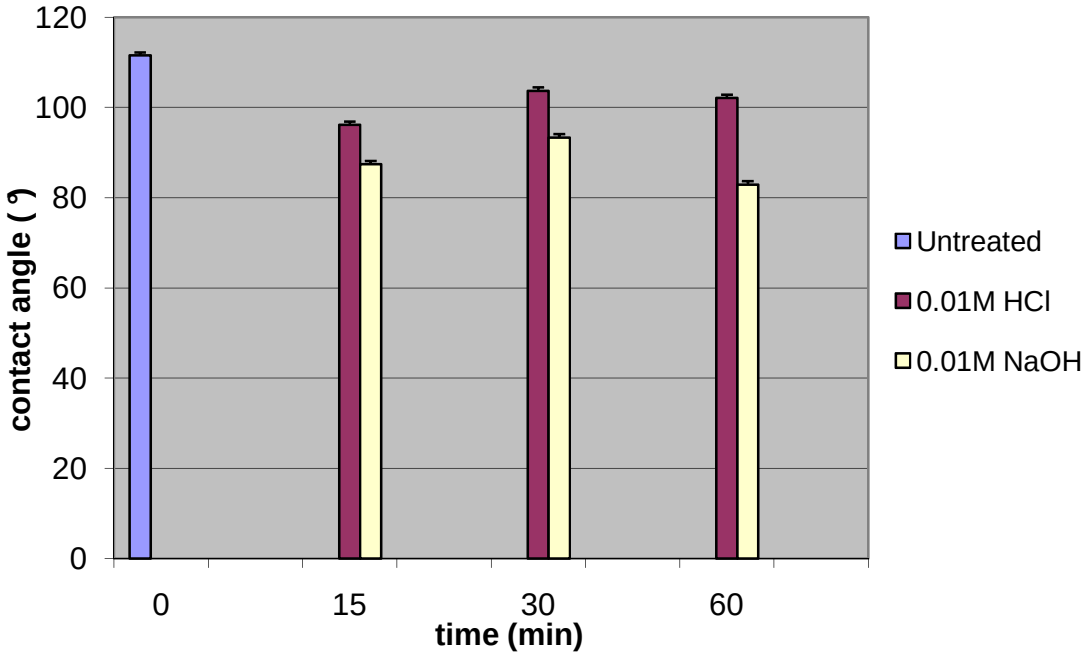

4.3 Protein immobilized electrospun nanofibers

Surface functionalization procedures for PLLA and hybrid nanofibers are shown in Figure3.2. Hydrophilic primary amine groups in a copolymer will make a hybrid mat more hydrophilic. As hydrogen bonds will form between the protons in water molecules and the lone electron pairs in the nitrogen atom in an amine group, the saturated water vapor treatment is used to exposed the amine groups on the fiber surface. These amine groups will be conjugated to carboxyl groups in Rhodamine-BSA via crosslinking with EGS. When the fiber mats have been treated briefly with NaOH,

surface hydrolysis functions to turn hydroxyl groups on the PLLA fiber surface into carboxylic groups [6], which can then be conjugated to the amine groups in FITC-BSA via crosslinking using EDC and/or NHS.

SEM images of electrospun PLLA and hybrid nanofibers immobilized with Bovine Serum Albumin (BSA) are shown in Figure 4.5. The fiber surfaces become coarse and beads appear on the surfaces after reactions with protein. It also shows that the hybrid fibers swell and their diameter increase for about 1μm after reacting in aqueous solution for 2 hours, due to the increased hydrophilicity and water solubility of the PEG block. Swelling was also observed from PLLA nanofibers after BSA conjugation, this effect may be more obvious in cases of increased hydrophilicity after surface hydrolysis and multiple deposition of BSA. FITC-BSA and Rhodamine-BSA are used to provide a clearer view of the distribution of proteins that have been conjugated onto the fiber surfaces. CLSM images of BSA-loaded nanofibers were shown in Figure 4.6 and Figure 4.7. PLLA nanofibers immobilized with one layer of FITC-BSA (Figure 4.6) exhibit strong fluorescence on the surface of the fibers, giving a clear, fluorescence-free channel inside of the fiber. This proves that the protein has successfully immobilized on the surface of PLLA nanofibers. CLSM images for hybrid nanofibers immobilized with both FITC-BSA and Rhodamine-BSA are shown in Figure4.7. Both green (Figure 4.7A, FITC excitation wavelength at 488nm) and red (Figure 4.7B, Rhodamine B excitation wavelength at 540nm) fluorescence appear on the surface of hybrid nanofibers. Figure 4.7Cis the overlapped image showing two fluorescence dye-labeled BSAs, the overlapping area giving a yellow-orange color. The results suggest that different protein molecules can be efficiently immobilized onto the surface of hybrid nanofibers. Such

functional nanofibers are potentially useful and important in the development of nanofibrous wound dressings or tissue engineering scaffolds, because they make it possible to immobilize different growth factors on the nanofiber substrate to promote wound healing or tissue regeneration.

Figure 4.5 SEM micrographs of BSA conjugated nanofibers

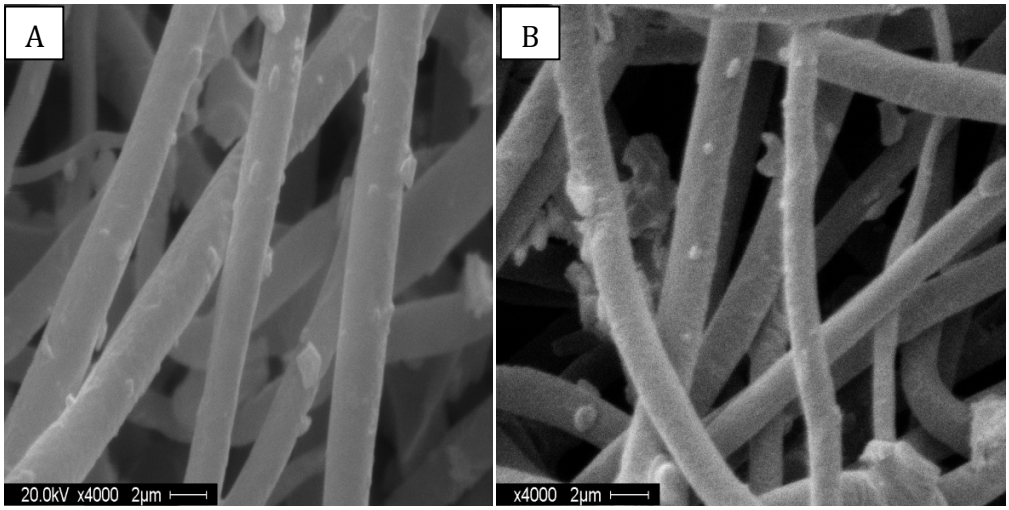

A: PLLA-BSA, B: hybrid-2BSA

Figure4.6 Confocal image of PLLA nanofibers immobilized with FITC-BSA

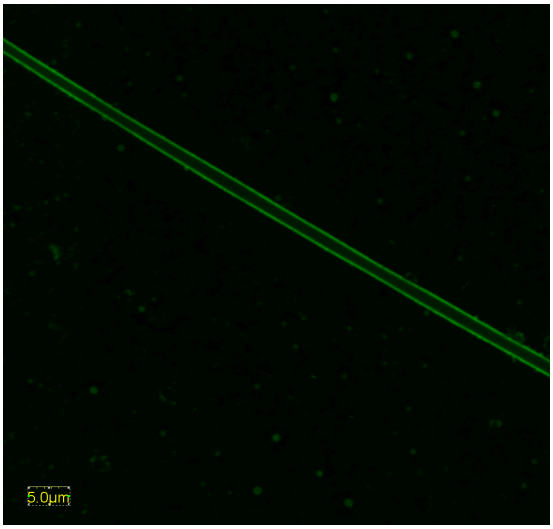

Figure4.7 Confocal images of hybrid nanofibers immobilized with FITC-BSA and Rhodamine-BSA

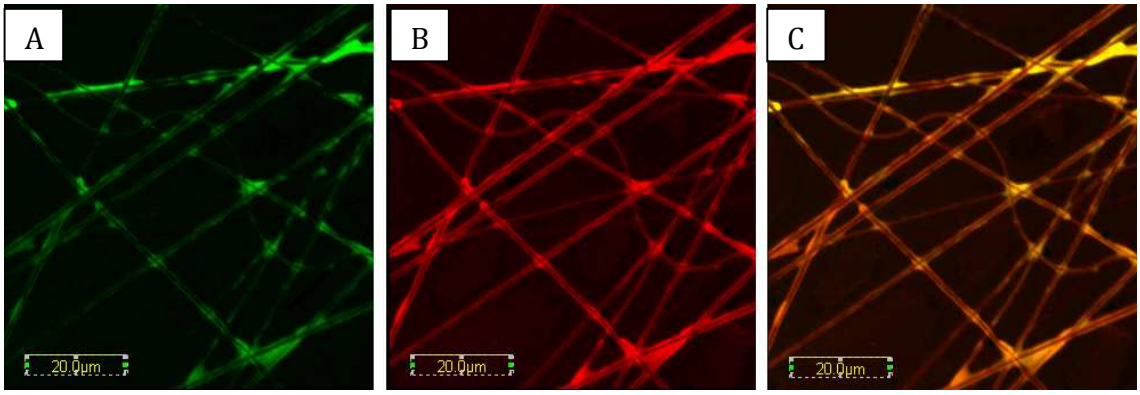

A: hybrid nanofibers immobilized with FITC-BSA, B: hybrid nanofibers immobilized with Rhodamine-BSA, C: hybrid nanofibers immobilized with both FITC-BSA and Rhodamine-BSA

4.4 Secondary structure of immobilized BSA

FTIR-ATR is used to detect the secondary structure of protein on the fiber surface. The surface functionalization procedures of PLLA and hybrid nanofibers are shown in Figure3.2. After pre-treating with NaOH, the carboxylic groups are supposed to be exposed to the surface of nanofibers [6], EDC, NHS and EGS all can help to conjugate protein to both amine groups and carboxylic groups, making it possible to immobilize two different layers of proteins. As shown in Figure 4.8, the amide I band showing in the protein backbone appears at 1642 cm^{-1}, the peak at 1454 cm^{-1} corresponding to the amide II vibration (N-H bending). C=O stretching of PLLA is shown as a strong peak at 1754 cm^{-1}. Figure 4.6 and 4.7 give the confocal images of surface functionalized PLLA and hybrid nanofibers. The fluorescence shown on the outer surface of each fiber also suggests that BSA has been successfully immobilized on the surface of the nanofibers.

Figure 4.8 ATR spectra of hybrid-2BSA nanofibrous mat

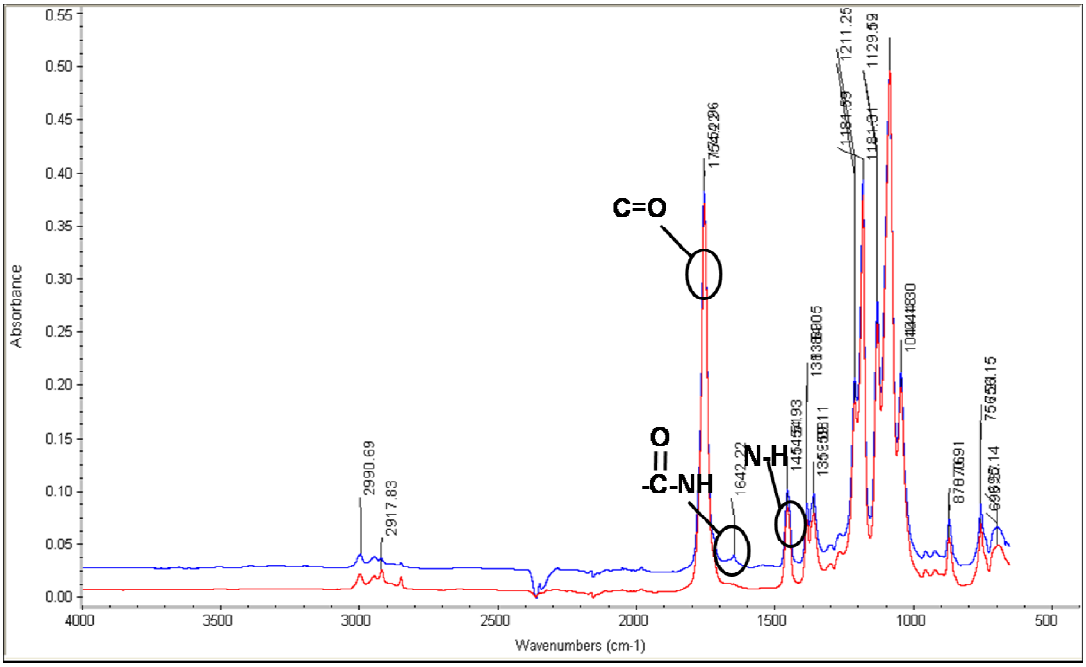

4.5 The amount of BSA immobilized on PLLA and hybrid nanofibrous mat

Since the BSA immobilized PLLA and hybrid nanofibrous mat does not dissolve easily in any common solvent like chloroform or methanol, and tends to form micelles, it is not possible to determine the amount of BSA immobilized by dissolving the sample in chloroform and check the protein absorption of protein using UV-vis spectrometer. Accordingly, the amount of BSA immobilized is calculated by deducting the amount of BSA left in the solution from the total amount of BSA added. The total amount of BSA immobilized on PLLA and hybrid nanofibrous mat is shown in Table 4.2. By comparing P3-2&P6-2; H3-2&H6-2 and H3-3&H6-3, it can be seen that the amount of TCH incorporated in the nanofibers does not influence the amount of BSA immobilized on the nanofibers. The hybrid nanofibrous mats immobilized with two layers of BSA (H3-3,

H6-3) almost double the amount of BSA immobilized on PLLA nanofibrous mats (P3-2) and hybrid mats with one layer of BSA immobilized on them(H3-2, H6-2). This implies that the amount of BSA that can be immobilized on the mats is only influenced by the amount of active amine groups and carboxylic groups which can react with BSA.

Table 4.2 Amount of BSA (ug) immobilized on nanofibrous mats

	P3-2	P6-2	H3-2	H3-3	H6-2	H6-3
Immobilized BSA (ug/5mg mat)	3469±112	3416±18	3913±82	6962±151	4197±57	7509±78

4.6 In vitro release of Tetracycline hydrochloride (TCH)

The release profiles of the incorporated TCH in electrospun PLLA and hybrid nanofibers are shown in Figure 4.10 and Figure 4.11. It can be seen that the rate of TCH release decrease with increased TCH content in the fiber. This phenomenon was also reported in our previous work[160]. Briefly, in emulsion electrospinning, TCH is incorporated into nanofibers to form a reservoir-type core/sheath structure: the higher amount of TCH in the emulsion, the thinner core and the thicker sheath of fibers will be. The formation of a core-sheath structure includes the de-emulsification of drug solution induced by stretching and solvent evaporation. Due to the high degree of de-

emulsification of the aqueous droplet with higher TCH concentration, a slower release rate of TCH from the nanofibers can be observed.

On the other hand, the polymer solvent, chloroform, is more volatile than water in which the TCH was dissolved. As a result, when water evaporates during the formation of nanofibers, it may leave behind nanopores or nano channels in the structure of the fibers. According to the desorption-limited mechanism of drug release from polymer nanofibers [161], drugs that have been deposited in such nanopores may get quickly released upon contact with an aqueous bath. This may explain the initial burst release of drugs from nanofibers in the drug release profiles: TCH undergoes a burst release from both PLLA and hybrid nanofibrous mats, nearly 70μg TCH being released during the first 48 hours. The drug is then released at a stable and constant rate during the next 100 hours for both PLLA and hybrid nanofibrous mats. After 48 hours, the release rate of TCH from PLLA nanofibers slowed down dramatically: accumulative releases of drugs reach only 95μg for 3%TCH-loaded and 75μg for 6%TCH-loaded PLLA nanofibers respectively and accumulative drug releases are 85μg for 3%TCH-loaded and 80μg for 6%TCH-loaded hybrid nanofibrous mat respectively. This can be explained by the slow hydrolysis and degradation of the polymer [162].

Comparing the profiles of drug release from PLLA and hybrid nanofibers, we find that TCH shows a slower rate of release from PLLA nanofibrous mat than from the hybrid mat. It has been suggested that the molecular weight also has an effect on the release rate [161]. Hybrid nanofibers can be electrospun from a combination of PLLA and PEG-PLLA-NH_2, and the copolymer's molecular weight is much smaller than PLLA. It's been

proved that a high molecular weight contributes to the lower nanoporosity of the fibers, which in turn decreases the overall rate of desorption of the drug from the surface.

The profiles of TCH released from PLLA and hybrid mats that have been conjugated with BSA are shown in Figure 4.12 and Figure 4.13. TCH is released gradually over time and no obvious burst release is observed. This is owing to the fact that the reaction with protein takes place in the aqueous solution, where the burst release of TCH has already occurred. Therefore, after surface functionalization with the proteins, profiles of the drug release become less steep, corresponding to the stage of stable drug release in Figures 4.10 and 4.11. It can also be noted that samples loaded with 6%TCH loading demonstrate a higher rate of drug release than the 3%TCH samples, reversing the trend as observed in the tests for samples without BSA. This may be caused by the effect of swelling of the nanofibers (Figure 4.5A and B) during the treatment, which facilitates the escape of drugs from nanofibers.

Figure 4.9 Release profiles of the TCH encapsulated PLLA nanofibrous mat

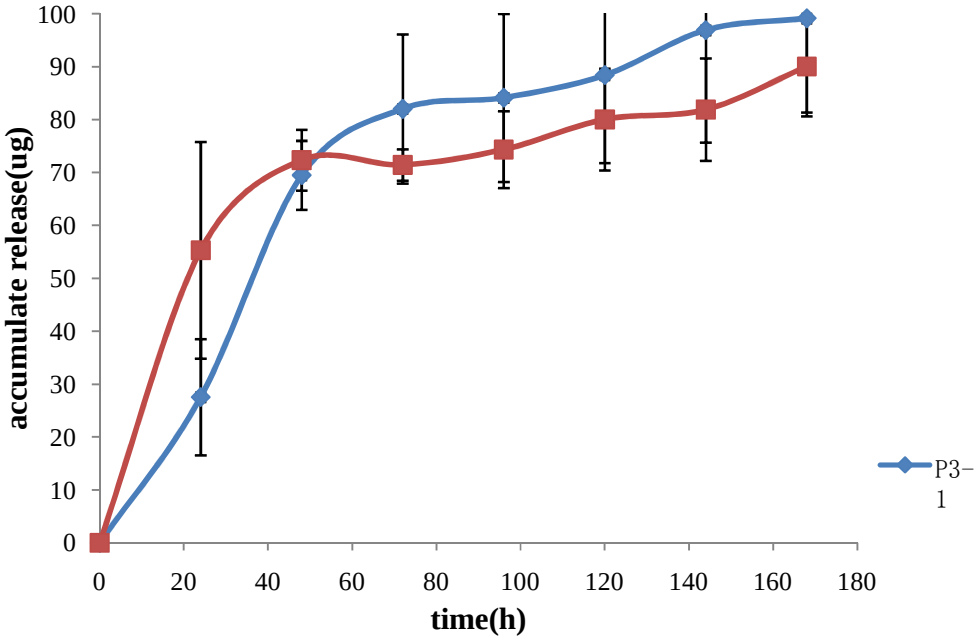

Figure 4.10 Release profiles of the TCH encapsulated hybrid nanofibrous mat

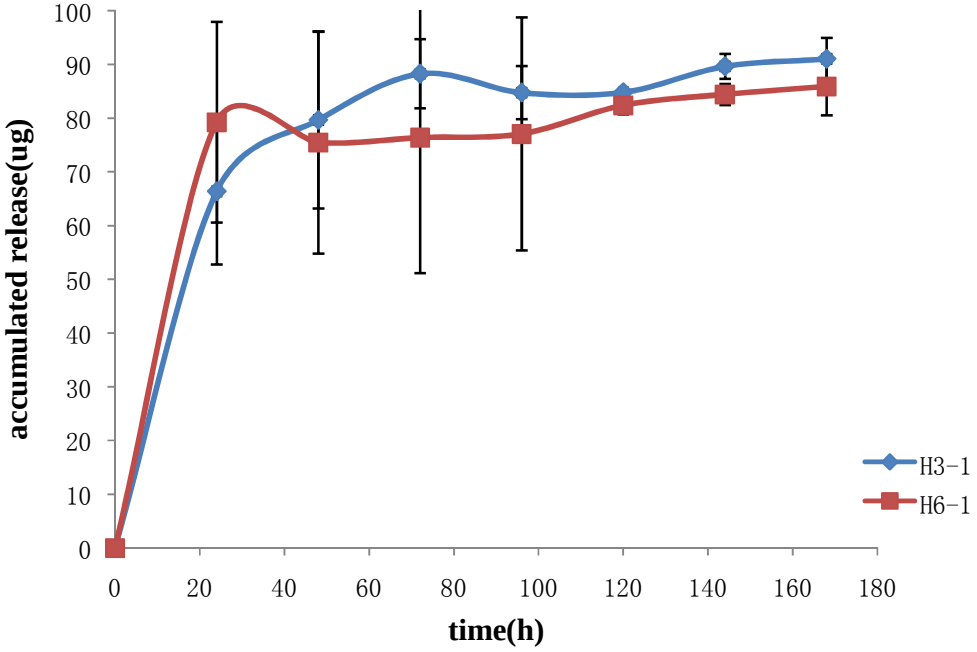

Figure 4.11 Profiles of release of TCH from the PLLA-BSA mat

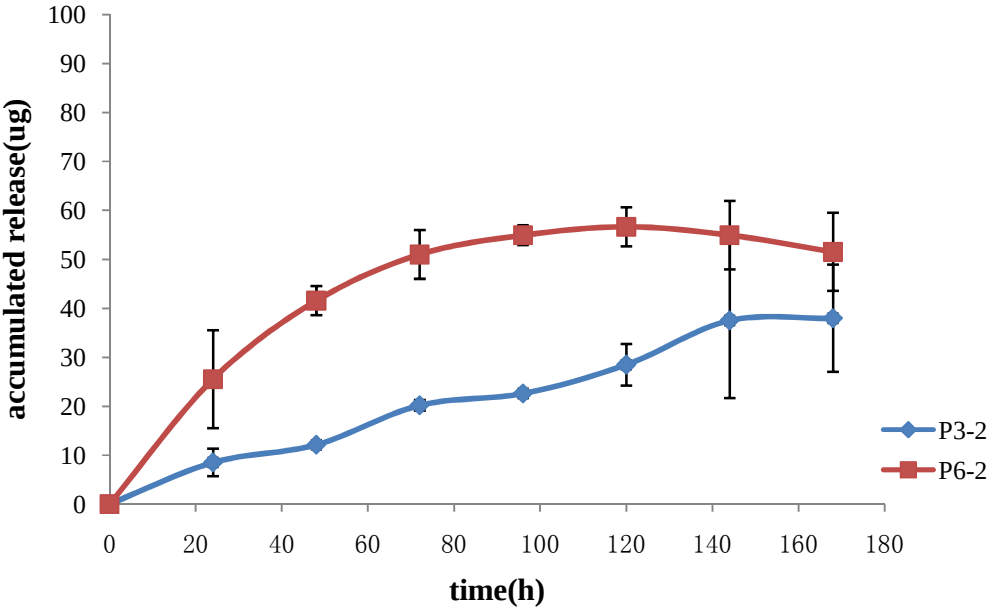

Figure 4.12 Profiles of release of TCH from the hybrid-2BSA mat

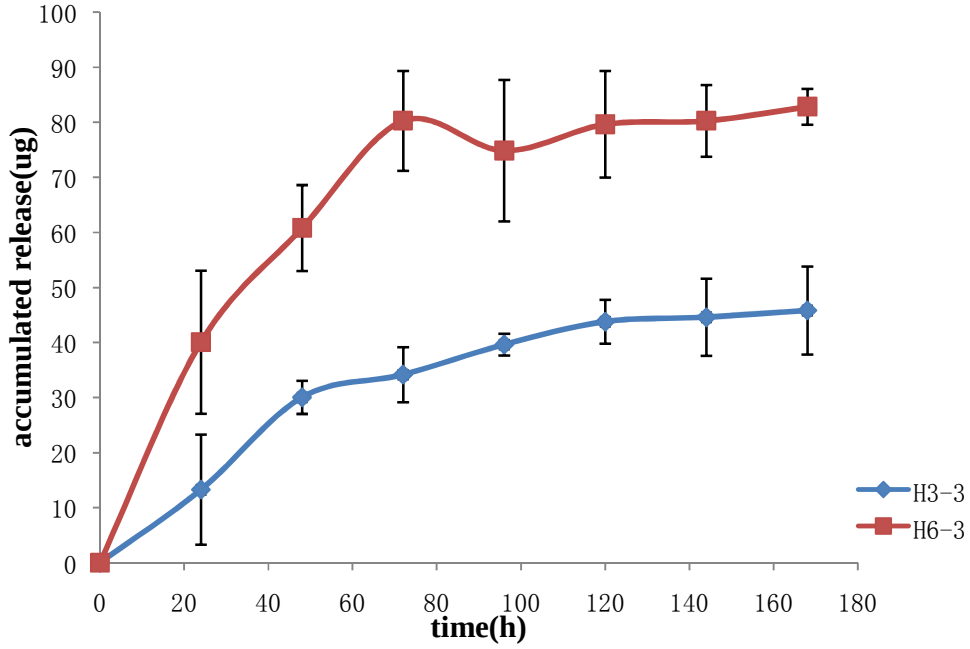

4.7 Anti-bacteria test

The anti-bacterial capacity of TCH-loaded nanofibers was evaluated using the microorganism susceptibility test. The impact of protein immobilization on the antibacterial ability of drug-loaded nanofibers was also checked. The diameter of the inhibition zone was used to specify the anti-microbial capacity of the nanofiber samples. The results are shown in Figure 4.14. The control samples were prepared by dropping onto the blank mats an aqueous solution of TCH, the amount of which had been made to equal that in the TCH-loaded nanofibrous mats fabricated by emulsion electrospinning. Results of the paired t-test are listed in Table 4.3. It indicated that the inhibiting impact for the groups undergoing the treatment was significant.

It can be seen from Figure 4.14(A & B) that the anti-bacterial capacity of drug-loaded nanofibers lasts longer than the controls. The reason may be that the drugs were mainly adsorbed onto the surface of the nanofibers in the control samples. As a result, TCH released more rapidly (depleted in 4 days) than the emulsion electrospun TCH-loaded nanofibers (effective for 6-7 days), in which TCH was incorporated into the interior of the nanofibers and got released from its reservoir structure through a constant release process. It is also shown that samples loaded with 6% TCH by emulsion electrospinning exhibited a more prolonged anti-bacterial capacity than samples loaded with 3% TCH, since the total amount of TCH capsulated was higher. Figure 4.14 C and D show the anti-microbial capacity of TCH-loaded PLLA and hybrid mats respectively after surface functionalization with BSA: size of the inhibition zone decreases with time, and the anti-bacterial capability of medicated nanofibers lasts 7 days for the PLLA-BSA samples, and only 3 days for the hybrid-2BSA samples. This can be explained by the

surface functionalization processes in which the treatment took place in the aqueous environment to result in a loss of drug. The hybrid samples twice under went the process of immobilization of BSA, leading to a larger TCH loss. However, this drug loss could be compensated by the incorporation of a larger amount of the drug in the future work.

Table 4.3 Inhibition zone t-test analysis

	P3-1/P3-1 control	P6-1/P6-1 control	H3-1/H3-1 control	H6-1/H6-1 control	P3-2/P6-2	H3-3/H6-3
Day1	**	**	**	*	**	**
Day2	**	**	**	**	**	*
Day3	**	**	**	**	**	*
Day4	**	**	**	**	**	
Day5	**	**	**	**	**	
Day6	**	**	**	**	**	
Day7	**	**	**	**	**	

*: 1%<p<5%

**: p<1%

Figure 4.13 Anti-microbial test

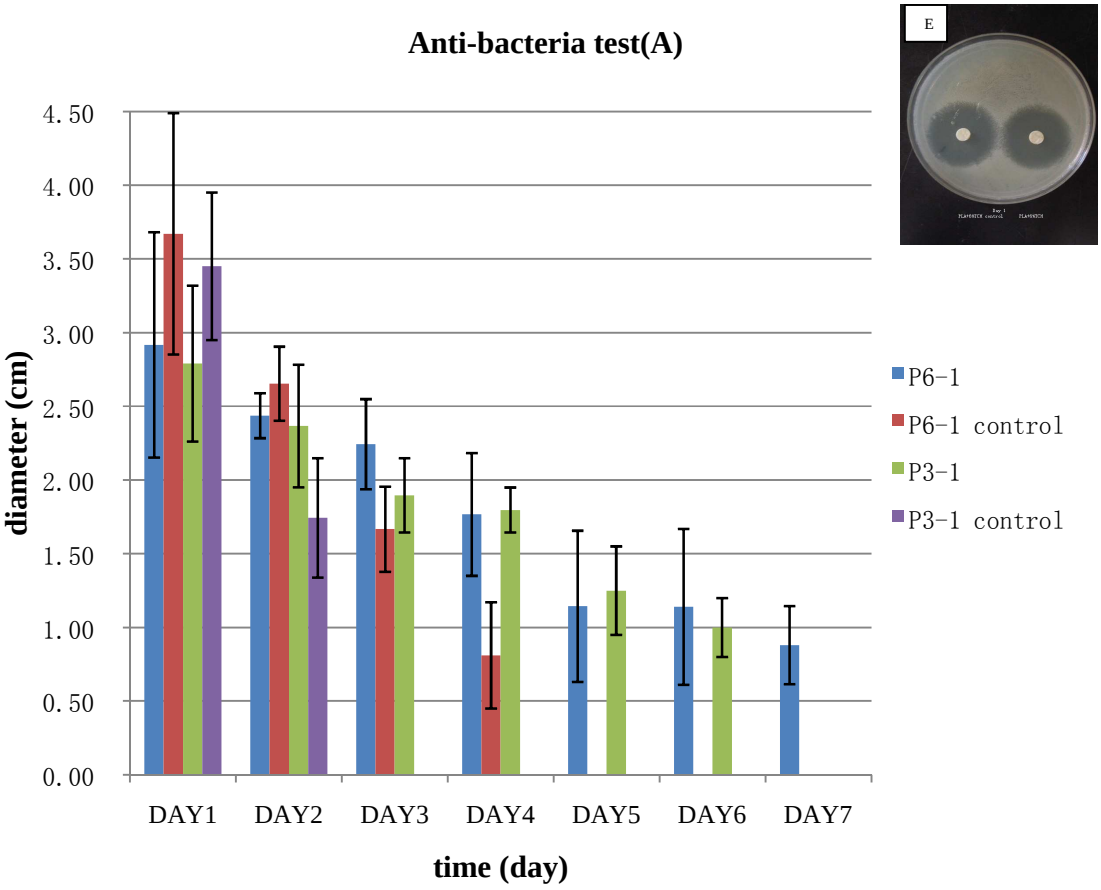

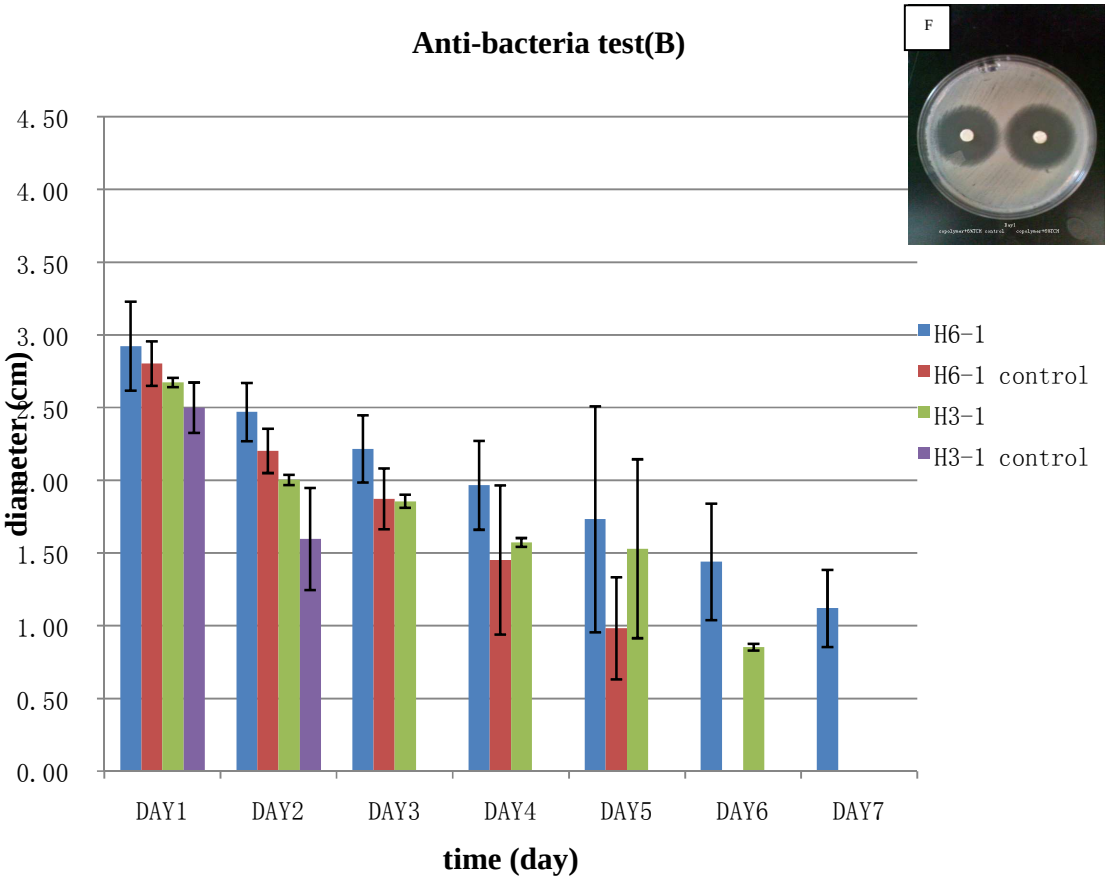
Anti-bacteria test(B)
F
4.50
4.00
3.50
3.00
2.50
2.00
1.50
1.00
0.50
0.00
diameter(cm)
DAY1
DAY2
DAY3
DAY4
DAY5
DAY6
DAY7
time (day)
H6-1
H6-1 control
H3-1
H3-1 control

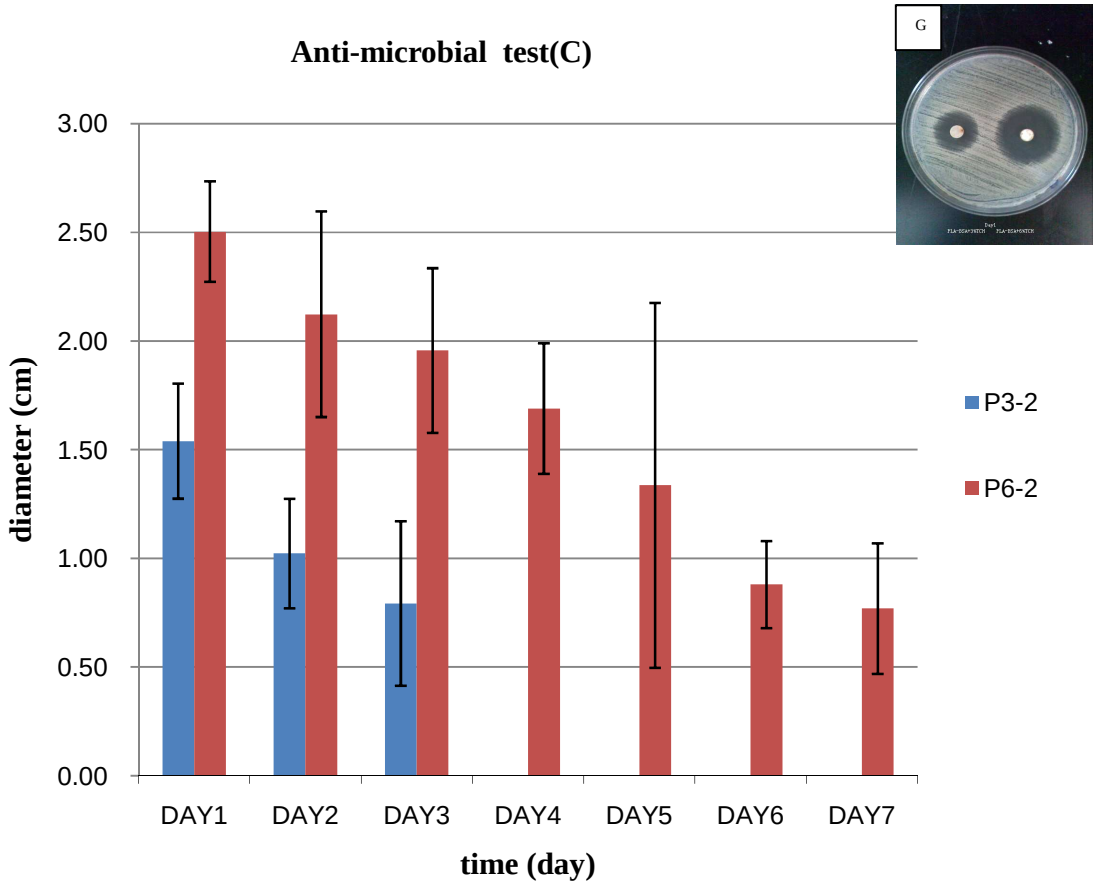
Anti-microbial test(C)
G
3.00
2.50
2.00
1.50
1.00
0.50
0.00
diameter (cm)
DAY1
DAY2
DAY3
DAY4
DAY5
DAY6
DAY7
time (day)
P3-2
P6-2

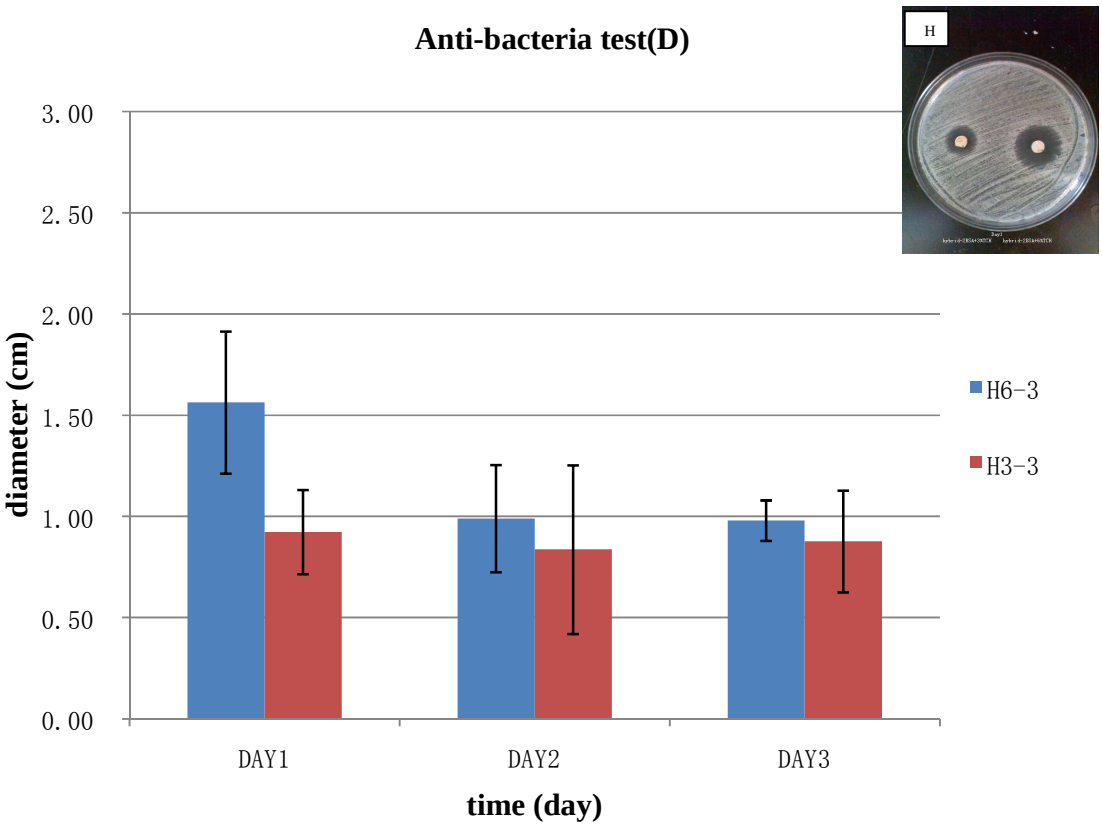

A: TCH loaded PLA nanofibrous mat, B: TCH loaded hybrid nanofibrous mat, C: TCH loaded PLA-BSA nanofibrous mat, D: TCH loaded hybrid-2BSA nanofibrous mat, E: P6-1 and P6-1control disks in Day1, F: H6-1 and H6-1 control disks in Day1, G: P3-2 and P6-2 disks in Day1, H: H3-3 and H6-3 disks in Day1

Figure 4.14 Sampling anti-bacteria disks of H6-1

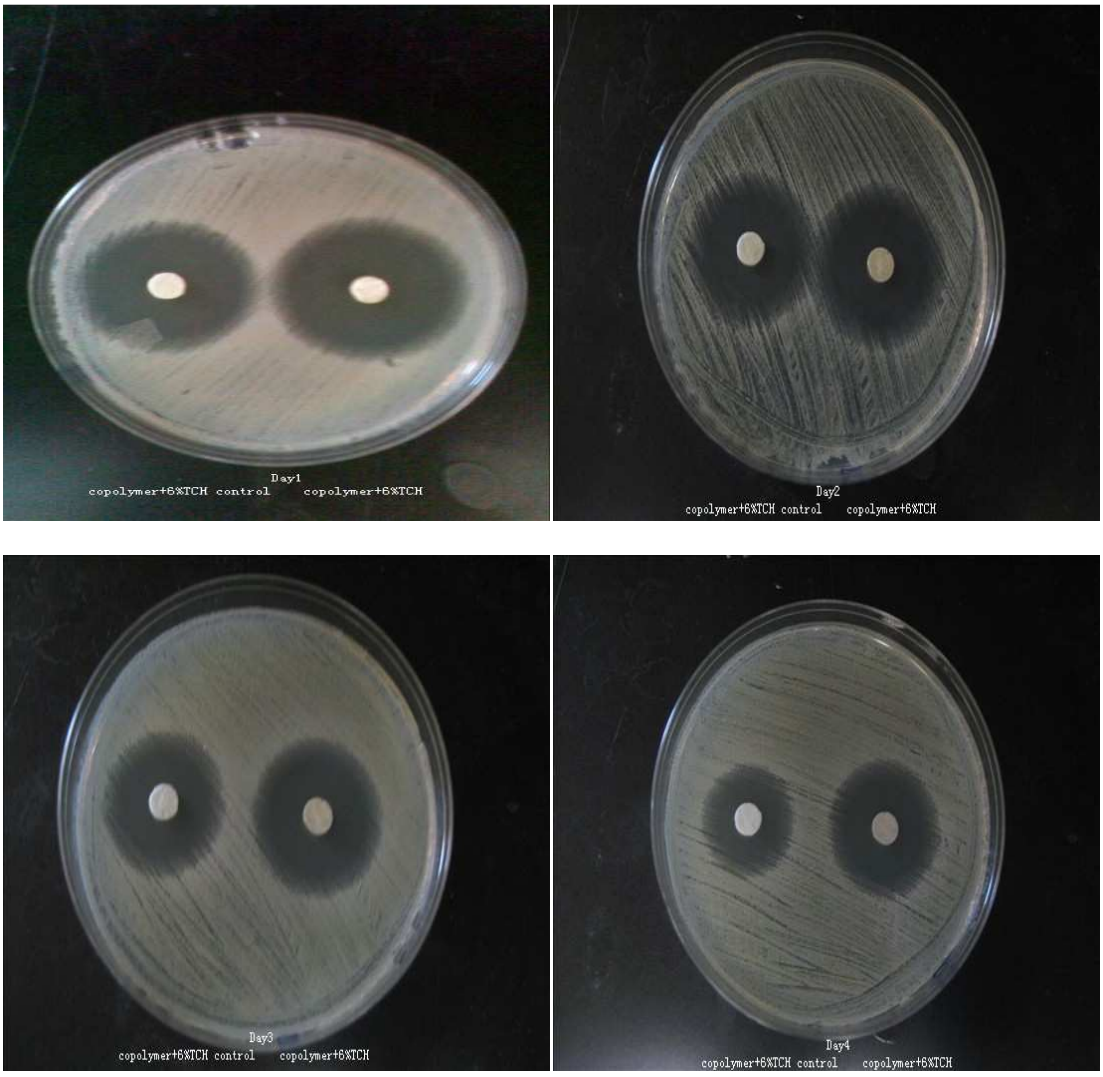


Day5
copolymer+6%TCH control
copolymer+6%TCH


Day6
copolymer+6%TCH control
copolymer+6%TCH


Day7
copolymer+6%TCH

Chapter 5 Conclusion and Future Studies

This chapter will give a brief conclusion on this study, discuss the potential applications of the developed functional nanofibers. Further work on this study will also be suggested.

5.1 Conclusion

In this study, we developed multi-functional nanofibers that were incorporated with an antibacterial agent and immobilized with two different proteins. TCH, a model antibiotic drug, was loaded into the PLLA and hybrid PLLA/PLLA-PEG nanofibers by emulsion electrospinning. Fluorescein was incorporated in the PLLA and hybrid nanofibers to provide a better view of the distributions of the drug in the nanofibers. A core-sheath structure was observed in the drug-loaded hybrid nanofibers, in which the polymer constitutes the sheath and the drug is incorporated in the core. Such core-sheath structure, however, was not found in the drug-loaded PLLA nanofibers, probably because of the difficulty in obtaining a stable emulsion for electrospinning.

The drug-loaded nanofibers were surface functionalized to provide functional groups (i.e. carboxylic groups and amine groups) that can be utilized to conjugate to BSA. SEM images showed that the BSA-immobilized nanofibers appeared to be thicker than original nanofibers, which may be caused by the swelling of nanofibers, and that the fiber surface also became slightly rougher after the reactions. The characteristic peaks of protein in the FTIR-ATR indicated that the secondary structure of the immobilized BSA has not been changed during the immobilization processes. Confocal images also confirmed the successful surface immobilization of BSA: one type of BSA (FITC-BSA) can be

immobilized onto the PLLA nanofibers, while two types of BSA (FITC-BSA and Rhodamine-BSA)) can be immobilized onto the surface of hybrid PLLA/PLLA-PEG nanofibers. Such functional nanofibers are potentially useful and important in the development of nanofibrous wound dressings or tissue engineering scaffolds, because they make it possible to immobilize different growth factors to promote wound healing or tissue regeneration.

The release profiles showed a sustained release of the drug from the drug-loaded nanofibers, starting with a initial burst-release of TCH that may have been loosely deposited in the nanopores on the fiber surface, followed by a slow and constant release of the drug into the media which can be caused by the polymer's hydrolysis and slow degradation. As to the nanofibers conjugated with BSA, there has been no burst release observed for both PLLA and hybrid mats. This is owing to the fact that the reaction with protein takes place in the aqueous solution, where the burst release of TCH has already occurred. The swelling effect may have cause the drug to release faster.

Anti-bacterial tests showed that the antibacterial effect of drug-loaded nanofibers lasted longer than that of the controls. The nanofibers loaded with 6% TCH exhibited a more prolonged antibacterial capacity than the nanofibers loaded with 3%TCH. After surface functionalization with BSA, antibacterial capacity for both PLLA and hybrid nanofibers decreased. This may be caused by the loss of drug during the reactions in an aqueous environment. However, this drug loss can be compensated by the incorporation of a larger amount of the drug.

5.2 Future Studies

In the future studies for this research, growth factors or other bioactive molecules that can stimulate cellular proliferation and differentiations will be used for the functionalization of nanofibers. In vitro cytotoxicity assay and cell migration tests will be performed to evaluate the functionalized nanofibrous mats for their potential applications in wound healing. Normal human dermal fibroblast (NHDF) can be seeded onto the functionalized nanofibers to evaluate the bioactivity of the immobilized proteins. Fibroblast is a type of cells responsible for synthesizing extracellular matrix and collagen, which is the structural framework for human tissues, and also plays a critical role in wound healing process. Fluorescence microscope will be used to monitor the migration of NHDFs and the development of cytoskeleton on the growth factor-immobilized PLLA and hybrid nanofibrous mats. We will also address the issue of drug loss during immobilization of protein onto nanofibers in the aqueous environment by increasing the amount of the drug in the emulsion process.

References

1. Okuda, T., K. Tominaga, and S. Kidoaki, *Time-programmed dual release formulation by multilayered drug-loaded nanofiber meshes.* Journal of Controlled Release, 2010. **143**(2): p. 258-264.
2. Kim, K., et al., *Incorporation and controlled release of a hydrophilic antibiotic using poly(lactide-co-glycolide)-based electrospun nanofibrous scaffolds.* Journal of Controlled Release, 2004. **98**(1): p. 47-56.
3. Xu, X.L., et al., *Ultrafine PEG-PLA fibers loaded with both paclitaxel and doxorubicin hydrochloride and their in vitro cytotoxicity.* European Journal of Pharmaceutics and Biopharmaceutics, 2009. **72**(1): p. 18-25.
4. Xie, J. and C.H. Wang, *Electrospun micro- and nanofibers for sustained delivery of paclitaxel to treat C6 glioma in vitro.* Pharmaceutical Research, 2006. **23**(8): p. 1817-1826.
5. Ignatious, F., et al., *Electrospun Nanofibers in Oral Drug Delivery.* Pharmaceutical Research, 2010. **27**(4): p. 576-588.
6. Patel, S., et al., *Bioactive nanofibers: Synergistic effects of nanotopography and chemical signaling on cell guidance.* Nano Letters, 2007. **7**(7): p. 2122-2128.
7. Taek Gyoung Kim and T.G. Park, *Surface Functionalized Electrospun Biodegradable Nanofibers for Immobilization of Bioactive Molecules.* Biotechnology Progress, 2006. **22**(4): p. 1108-1113.
8. Qi, H., et al., *Encapsulation of drug reservoirs in fibers by emulsion electrospinning: Morphology characterization and preliminary release assessment.* Biomacromolecules, 2006. **7**(8): p. 2327-2330.
9. Ji, W., et al., *Fibrous scaffolds loaded with protein prepared by blend or coaxial electrospinning.* Acta Biomaterialia. **In Press, Uncorrected Proof**.
10. Yan, S., et al., *Poly(l-lactide-co-[var epsilon]-caprolactone) electrospun nanofibers for encapsulating and sustained releasing proteins.* Polymer, 2009. **50**(17): p. 4212-4219.
11. Lee, J.H., et al., *Stable and continuous long-term enzymatic reaction using an enzyme-nanofiber composite.* Applied Microbiology and Biotechnology, 2007. **75**(6): p. 1301-1307.
12. Zhu, Y., et al., *Esophageal epithelium regeneration on fibronectin grafted poly(l-lactide-co-caprolactone) (PLLC) nanofiber scaffold.* Biomaterials, 2007. **28**(5): p. 861-868.
13. Albritton, J.S., *Complications of wound repair.* Clinics in podiatric medicine and surgery, 1991. **8**(4): p. 773-785.
14. Tepelidis, N.T., *Wound healing in the elderly.* Clinics in podiatric medicine and surgery, 1991. **8**(4): p. 817-826.
15. Wilczynski, R.J., *Complications of foot surgery. Wound dehiscence, hypertrophic scars, and keloids.* Clinics in podiatric medicine and surgery, 1991. **8**(2): p. 359-365.

16. Van, F.B.L. and T.K. Hunt, *Oxygen and wound healing.* Clin. Plast. Surg, 1990. **17**: p. 463-469.
17. Hanna, J.R. and J.A. Giacopelli, *A review of wound healing and wound dressing products.* The Journal of Foot and Ankle Surgery. **36**(1): p. 2-14.
18. Canter, K.G., *Conservative management of wounds.* Clinics in podiatric medicine and surgery, 1991. **8**(4): p. 787-798.
19. Sipos P, et al., *Special wound healing methods used in ancient Egypt and the mythological background.* World J Surg 2004. **28**(2): p. 211–6.
20. Rogers AA, et al., *Adsorption of serum-derived proteins by primary dressings: implications for dressing adhesion to wounds.* J Wound Care 1999. **8**(8): p. 403–6.
21. MS, A., *Four alginate dressings in the treatment of partial thickness wounds: a comparative experimental study.* Br J Plast Surg 1996. **49**(2): p. 129-34.
22. Jiong, C., et al., *Randomized controlled trial of the absorbency of four dressings and their effects on the evaporation of burn wounds.* Chinese Medical Journal, 2007. **120**(20): p. 1788-1791.
23. Khil, M.S., et al., *Electrospun nanofibrous polyurethane membrane as wound dressing.* Journal of Biomedical Materials Research Part B-Applied Biomaterials, 2003. **67B**(2): p. 675-679.
24. Powell, H.M., D.M. Supp, and S.T. Boyce, *Influence of electrospun collagen on wound contraction of engineered skin substitutes.* Biomaterials, 2008. **29**(7): p. 834-843.
25. Rho, K.S., et al., *Electrospinning of collagen nanofibers: Effects on the behavior of normal human keratinocytes and early-stage wound healing.* Biomaterials, 2006. **27**(8): p. 1452-1461.
26. Howling, G.I., et al., *The effect of chitin and chitosan on the proliferation of human skin fibroblasts and keratinocytes in vitro.* Biomaterials, 2001. **22**(22): p. 2959-2966.
27. Rao, S.B. and P.S. Chandra, *Use of chitosan as a biomaterial: Studies on its safety and hemostatic potential.* Journal of Biomedical Materials Research, 1997. **34**(1): p. 21-28.
28. Diegelmann, R.F., et al., *Analysis of the effects of chitosan on inflammation, angiogenesis, fibroplasia, and collagen deposition in polyvinyl alcohol sponge implants in rat wounds.* Wound Repair and Regeneration, 1996. **4**(1): p. 48-52.
29. Okamoto, Y., et al., *Evaluation of chitin and chitosan on open would healing in dogs.* The Journal of veterinary medical science / the Japanese Society of Veterinary Science, 1995. **57**(5): p. 851-854.
30. Lip Yong, C., et al., *Biocompatibility of potential wound management products: Fungal mycelia as a source of chitin/chitosan and their effect on the proliferation of human F1000 fibroblasts in culture.* Journal of Biomedical Materials Research, 1994. **28**(4): p. 463-469.
31. Min, B.M., et al., *Chitin and chitosan nanofibers: electrospinning of chitin and deacetylation of chitin nanofibers.* Polymer, 2004. **45**(21): p. 7137-7142.

32. Chen, J.P., G.Y. Chang, and J.K. Chen, *Electrospun collagen/chitosan nanofibrous membrane as wound dressing.* Colloids and Surfaces a-Physicochemical and Engineering Aspects, 2008. **313**: p. 183-188
704.
33. Lee, C.T., C.P. Huang, and Y.D. Lee, *Biomimetic porous scaffolds made from poly(L-lactide)-g-chondroitin sulfate blend with poly(L-lactide) for cartilage tissue engineering.* Biomacromolecules, 2006. **7**(7): p. 2200-2209.
34. Casper, C.L., et al., *Functionalizing electrospun fibers with biologically relevant macromolecules.* Biomacromolecules, 2005. **6**(4): p. 1998-2007.
35. Roh, D.H., et al., *Wound healing effect of silk fibroin/alginate-blended sponge in full thickness skin defect of rat.* Journal of Materials Science-Materials in Medicine, 2006. **17**(6): p. 547-552.
36. Kobayashi, H., *Surface modified poly(vinyl alcohol) nanofiber for the artificial corneal stroma.* ASBM7: Advanced Biomaterials VII, 2007. **342-343**: p. 209-212
964.
37. Rujitanaroj, P.O., N. Pimpha, and P. Supaphol, *Wound-dressing materials with antibacterial activity from electrospun gelatin fiber mats containing silver nanoparticles.* Polymer, 2008. **49**(21): p. 4723-4732.
38. Xu, X.L. and M.H. Zhou, *Antimicrobial gelatin nanofibers containing silver nanoparticles.* Fibers and Polymers, 2008. **9**(6): p. 685-690.
39. Kyung Hwa, H., *Preparation and properties of electrospun poly(vinyl alcohol)/silver fiber web as wound dressings.* Polymer Engineering & Science, 2007. **47**(1): p. 43-49.
40. Maneerung, T., S. Tokura, and R. Rujiravanit, *Impregnation of silver nanoparticles into bacterial cellulose for antimicrobial wound dressing.* Carbohydrate Polymers, 2008. **72**(1): p. 43-51.
41. Duan, Y.-y., et al., *Preparation of antimicrobial poly(ε-caprolactone) electrospun nanofibers containing silver-loaded zirconium phosphate nanoparticles.* Journal of Applied Polymer Science, 2007. **106**(2): p. 1208-1214.
42. Formhals, A., *US Patent 1975504*. 1934.
43. Seeram Ramakrishna, K.F., Wee-Eong Teo, Teik-Cheng Lim, Zuwei Ma, *An Introduction to Electrospinning and Nanofibers*. 2005: World Scientific Publishing Co. Pte. Ltd.
44. Formhals, A., *US Patent 2160962*. 1939.
45. Formhals, A.U., *US Patent 2187306*. 1940.
46. Taylor, G.I., Proc Roy Soc London, 1969. **Volume A313**: p. 453.
47. Buchko, C.J., et al., *Processing and microstructural characterization of porous biocompatible protein polymer thin films.* Polymer, 1999. **40**(26): p. 7397-7407.
48. Baumgarten, P.K., JColloid Interface Sci, 1971. **36**: p. 71.
49. Larrondo, L. and R.S.J. Mandley, J Polym Sci: Polymer Physics 1981a. **Volume 19**: p. 909.
50. Larrondo, L. and R.S.J. Mandley, J Polym Sci: Polymer Physics 1981b. **Volume 19**: p. 921.

51. Larrondo, L. and R.S.J. Mandley, J Polym Sci: Polymer Physics 1981c. **Volume 19**: p. 933.
52. Hayati, I., A.I. Bailey, and T.F. Tadros, *Investigations into the mechanisms of electrohydrodynamic spraying of liquids. I. Effect of electric field and the environment on pendant drops and factors affecting the formation of stable jets and atomization.* J Colloid Interface Sci 1987. **117**: p. 205.
53. Doshi, J. and D.H. Reneker, *Electrospinning process and applications of electrospun fibers.* Journal of Electrostatics, 1995. **35**(2-3): p. 151-160.
54. Reneker, D.H. and I. Chun, *Nanometre diameter fibres of polymer, produced by electrospinning.* Nanotechnology, 1996. **7**(3): p. 216-223.
55. Deitzel, J.M., et al., C Polymer, 2001. **42**: p. 261.
56. Deitzel, J.M., et al., C Polymer, 2001. **42**: p. 8163.
57. P. W. Gibson, H. L. Schreuder-Gibson, and D. Rivin, *Electrospun fiber mats: Transport properties.* AIChE Journal, 1999. **45**(1): p. 190-195.
58. Warner, S.B., et al., National Textile Center Annu Report, 1998. **November**: p. 83.
59. Moses, M., et al., Phys Fluids 2001. **13**: p. 2201.
60. Teo, W.E., et al., *Porous tubular structures with controlled fibre orientation using a modified electrospinning method.* Nanotechnology, 2005. **16**(6): p. 918-924.
61. Fennessey, S.F. and R.J. Farris, *Fabrication of aligned and molecularly oriented electrospun polyacrylonitrile nanofibers and the mechanical behavior of their twisted yarns.* Polymer, 2004. **45**(12): p. 4217-4225.
62. Pan, H., et al., *Continuous aligned polymer fibers produced by a modified electrospinning method.* Polymer, 2006. **47**(14): p. 4901-4904.
63. Gupta, P., et al., *In Situ Photo-Cross-Linking of Cinnamate Functionalized Poly(methyl methacrylate-co-2-hydroxyethyl acrylate) Fibers during Electrospinning.* Macromolecules, 2004. **37**(24): p. 9211-9218.
64. Schultz, J.M., B.S. Hsiao, and J.M. Samon, *Structural development during the early stages of polymer melt spinning by in-situ synchrotron X-ray techniques.* Polymer, 2000. **41**(25): p. 8887-8895.
65. P. Gupta, et al., *Development of high-strength fibers from aliphatic polyketones by melt spinning and drawing.* Journal of Applied Polymer Science, 2001. **82**(7): p. 1794-1815.
66. Shenoy, S.L., et al., *Role of chain entanglements on fiber formation during electrospinning of polymer solutions: good solvent, non-specific polymer-polymer interaction limit.* Polymer, 2005. **46**(10): p. 3372-3384.
67. Zong, X., et al., *Structure and process relationship of electrospun bioabsorbable nanofiber membranes.* Polymer, 2002. **43**(16): p. 4403-4412.
68. Kameoka, J., et al., *A scanning tip electrospinning source for deposition of oriented nanofibres.* Nanotechnology, 2003. **14**(10): p. 1124-1129.
69. Huang, J. and X.Y. Wu, *Effects of pH, salt, surfactant and composition on phase transition of poly(NIPAm/MAA) nanoparticles.* Journal of Polymer Science Part a-Polymer Chemistry, 1999. **37**(14): p. 2667-2676.

70. Lin, T., et al., *The charge effect of cationic surfactants on the elimination of fibre beads in the electrospinning of polystyrene.* Nanotechnology, 2004. **15**(9): p. 1375-1381.
71. Megelski, S., et al., *Micro- and nanostructured surface morphology on electrospun polymer fibers.* Macromolecules, 2002. **35**(22): p. 8456-8466.
72. Jarusuwannapoom, T., et al., *Effect of solvents on electro-spinnability of polystyrene solutions and morphological appearance of resulting electrospun polystyrene fibers.* European Polymer Journal, 2005. **41**(3): p. 409-421.
73. Zhao, S.L., et al., *Electrospinning of ethyl-cyanoethyl cellulose/tetrahydrofuran solutions.* Journal of Applied Polymer Science, 2004. **91**(1): p. 242-246.
74. Zhong, S., et al., *An aligned nanofibrous collagen scaffold by electrospinning and its effects on in vitro fibroblast culture.* Journal of Biomedical Materials Research Part A, 2006. **79A**(3): p. 456-463.
75. Xu, C.Y., et al., *Aligned biodegradable nanotibrous structure: a potential scaffold for blood vessel engineering.* Biomaterials, 2004. **25**(5): p. 877-886.
76. Huang, L., et al., *Generation of Synthetic Elastin-Mimetic Small Diameter Fibers and Fiber Networks.* Macromolecules, 2000. **33**(8): p. 2989-2997.
77. Zong, X., et al., *Electrospun fine-textured scaffolds for heart tissue constructs.* Biomaterials, 2005. **26**(26): p. 5330-5338.
78. Xiumei Mo and H.-J. Weber, *Electrospinning P(LLA-CL) Nanofiber: A Tubular Scaffold Fabrication with Circumferential Alignment.* Macromolecular Symposia, 2004. **217**(1): p. 413-416.
79. Li, D., Y. Wang, and Y. Xia, *Electrospinning of Polymeric and Ceramic Nanofibers as Uniaxially Aligned Arrays.* Nano Letters, 2003. **3**(8): p. 1167-1171.
80. Kakade, M.V., et al., *Electric Field Induced Orientation of Polymer Chains in Macroscopically Aligned Electrospun Polymer Nanofibers.* Journal of the American Chemical Society, 2007. **129**(10): p. 2777-2782.
81. Chen, F., C.N. Lee, and S.H. Teoh, *Nanofibrous modification on ultra-thin poly(epsilon-caprolactone) membrane via electrospinning.* Materials Science & Engineering C-Biomimetic and Supramolecular Systems, 2007. **27**(2): p. 325-332.
82. Choi, J.S., et al., *The influence of electrospun aligned poly([var epsilon]-caprolactone)/collagen nanofiber meshes on the formation of self-aligned skeletal muscle myotubes.* Biomaterials, 2008. **29**(19): p. 2899-2906.
83. Zong, X., et al., *Control of structure, morphology and property in electrospun poly(glycolide-co-lactide) non-woven membranes via post-draw treatments.* Polymer, 2003. **44**(17): p. 4959-4967.
84. Esrafilzadeh, D., R. Jalili, and M. Morshed, *Crystalline Order and Mechanical Properties of As-Electrospun and Post-treated Bundles of Uniaxially Aligned Polyacrylonitrile Nanofiber.* Journal of Applied Polymer Science, 2008. **110**(5): p. 3014-3022.
85. Kidoaki, S., I.K. Kwon, and T. Matsuda, *Mesoscopic spatial designs of nano- and microfiber meshes for tissue-engineering matrix and scaffold based on*

newly devised multilayering and mixing electrospinning techniques. Biomaterials, 2005. **26**(1): p. 37-46.
86. Moghe, A.K. and B.S. Gupta, *Co-axial electrospinning for nanofiber structures: Preparation and applications.* Polymer Reviews, 2008. **48**(2): p. 353-377.
87. Li, D. and Y.N. Xia, *Direct fabrication of composite and ceramic hollow nanofibers by electrospinning.* Nano Letters, 2004. **4**(5): p. 933-938.
88. Bellan, L.M., E.A. Strychalski, and H.G. Craighead, *Electrospun DNA nanofibers.* Journal of Vacuum Science & Technology B, 2007. **25**(6): p. 2255-2257.
89. Li, M., et al., *Electrospun protein fibers as matrices for tissue engineering.* Biomaterials, 2005. **26**(30): p. 5999-6008.
90. Li, J., et al., *Gelatin and Gelatin−Hyaluronic Acid Nanofibrous Membranes Produced by Electrospinning of Their Aqueous Solutions.* Biomacromolecules, 2006. **7**(7): p. 2243-2247.
91. Matthews, J.A., et al., *Electrospinning of Collagen Nanofibers.* Biomacromolecules, 2002. **3**(2): p. 232-238.
92. Matthews, J.A., et al., *Electrospinning of Collagen Type II: A Feasibility Study.* Journal of Bioactive and Compatible Polymers, 2003. **18**(2): p. 125-134.
93. Barnes, C.P., et al., *Nanofiber technology: Designing the next generation of tissue engineering scaffolds.* Advanced Drug Delivery Reviews, 2007. **59**(14): p. 1413-1433.
94. Sakabe, H., et al., *In vivo blood compatibility of regenerated silk fibroin.* Sen-i Gakkaishi, 1989. **45**: p. 487-490.
95. Min, B.-M., et al., *Electrospinning of silk fibroin nanofibers and its effect on the adhesion and spreading of normal human keratinocytes and fibroblasts in vitro.* Biomaterials, 2004. **25**(7-8): p. 1289-1297.
96. B.M. Min, et al., *Formation of silk fibroin matrices with different texture and its cellular response to normal human keratinocytes.* International Journal of Biological Macromolecules, 2004. **34**(5): p. 281-283.
97. Eugene D. Boland, et al., *Utilizing acid pretreatment and electrospinning to improve biocompatibility of poly(glycolic acid) for tissue engineering.* Journal of Biomedical Materials Research Part B: Applied Biomaterials, 2004. **71B**(1): p. 144-152.
98. Boland, E.D., et al., *Tailoring tissue engineering scaffolds using electrostatic procesing techniques: A study of poly(glycolic acid) electrospinning.* Journal of Macromolecular Science, Part A, 2001. **38**(12): p. 1231 - 1243.
99. Yang, F., et al., *Characterization of neural stem cells on electrospun poly(L-lactic acid) nanofibrous scaffold.* Journal of Biomaterials Science, Polymer Edition, 2004. **15**: p. 1483-1497.
100. Jing Zeng, et al., *Ultrafine fibers electrospun from biodegradable polymers.* Journal of Applied Polymer Science, 2003. **89**(4): p. 1085-1092.
101. Bognitzki., M., et al., *Submicrometer shaped polylactide fibers by electrospinning.* Abstracts of Papers of the American Chemical Society, 2000. **219**: p. U491-U491.

102. Jun, Z., et al., *Poly-L-lactide nanofibers by electrospinning - Influence of solution viscosity and electrical conductivity on fiber diameter and fiber morphology.* E-Polymers, 2003: p. -.
103. Chen-Ming Hsu and S. Shivkumar, *N,N-Dimethylformamide Additions to the Solution for the Electrospinning of Poly(ε-caprolactone) Nanofibers.* Macromolecular Materials and Engineering, 2004. **289**(4): p. 334-340.
104. Kousaku Ohkawa, et al., *Electrospun Non-Woven Fabrics of Poly(ε-caprolactone) and Their Biodegradation by Pure Cultures of Soil Filamentous Fungi.* Macromolecular Symposia, 2004. **216**(1): p. 301-306.
105. Ghasemi-Mobarakeh, L., et al., *Electrospun poly (epsilon-caprolactone) nanofiber mat as extracellular matrix.* Yakhteh, 2008. **10**(3): p. 179-184.
106. Rockwood, D.N., et al., *Electrospinning of a biodegradable polyurethane for use in tissue engineering.* Abstracts of Papers of the American Chemical Society, 2004. **228**: p. U364-U364.
107. Bin Ding, et al., *Preparation and characterization of a nanoscale poly(vinyl alcohol) fiber aggregate produced by an electrospinning method.* Journal of Polymer Science Part B: Polymer Physics, 2002. **40**(13): p. 1261-1268.
108. Yao, L., et al., *Electrospinning and Stabilization of Fully Hydrolyzed Poly(Vinyl Alcohol) Fibers.* Chemistry of Materials, 2003. **15**(9): p. 1860-1864.
109. Son, W.K., et al., *The effects of solution properties and polyelectrolyte on electrospinning of ultrafine poly(ethylene oxide) fibers.* Polymer, 2004. **45**(9): p. 2959-2966.
110. Mo, X.M., et al., *Electrospun P(LLA-CL) nanofiber: a biomimetic extracellular matrix for smooth muscle cell and endothelial cell proliferation.* Biomaterials, 2004. **25**(10): p. 1883-1890.
111. Kwon, I.K. and T. Matsuda, *Co-electrospun nanofiber fabrics of poly(L-lactide-co-epsilon-caprolactone) with type I collagen or heparin.* Biomacromolecules, 2005. **6**(4): p. 2096-2105.
112. Zhu, Y.B., et al., *Esophageal epithelium regeneration on fibronectin grafted poly(L-lactide-co-caprolactone) (PLLC) nanofiber scaffold.* Biomaterials, 2007. **28**(5): p. 861-868.
113. Casper, C.L., et al., *Functionalized electrospun fibers for potential use in biomedical applications.* Abstracts of Papers of the American Chemical Society, 2004. **228**: p. U515-U515.
114. Lunt, J., *Large-scale production, properties and commercial applications of polylactic acid polymers.* Polymer Degradation and Stability, 1998. **59**(1-3): p. 145-152.
115. Wong, W.H. and D.J. Mooney, *Synthetic Biodegradable Polymer Scaffold*. Synthesis and properties of biodegradable polymers used as synthetic matrices for tissue engineering, ed. A.A.e. al., Birhauser, Boston.
116. Kim, K., et al., *Control of degradation rate and hydrophilicity in electrospun non-woven poly(D,L-lactide) nanofiber scaffolds for biomedical applications.* Biomaterials, 2003. **24**(27): p. 4977-4985.

117. Yang, F., et al., *Electrospinning of nano/micro scale poly(L-lactic acid) aligned fibers and their potential in neural tissue engineering.* Biomaterials, 2005. **26**(15): p. 2603-2610.
118. Yang, F., et al., *Fabrication of nano-structured porous PLLA scaffold intended for nerve tissue engineering.* Biomaterials, 2004. **25**(10): p. 1891-1900.
119. Young You, et al., *In vitro degradation behavior of electrospun polyglycolide, polylactide, and poly(lactide-co-glycolide)* Journal of Applied Polymer Science, 2005. **95**(2): p. 193-200.
120. Lee, Y.H., et al., *Electrospun dual-porosity structure and biodegradation morphology of Montmorillonite reinforced PLLA nanocomposite scaffolds.* Biomaterials, 2005. **26**(16): p. 3165-3172.
121. Zhao, Y., X. Li, and X.Y. Yuan, *Synthesis of poly(ethylene glycol)-b-poly (L-lactic acid) diblock copolymers and formation of their electrospun fibers.* Acta Polymerica Sinica, 2008(5): p. 405-409.
122. Keun Kwon, I., S. Kidoaki, and T. Matsuda, *Electrospun nano- to microfiber fabrics made of biodegradable copolyesters: structural characteristics, mechanical properties and cell adhesion potential.* Biomaterials, 2005. **26**(18): p. 3929-3939.
123. Xu, C., et al., *Electrospun nanofiber fabrication as synthetic extracellular matrix and its potential for vascular tissue engineering.* Tissue Engineering, 2004. **10**(7-8): p. 1160-1168.
124. Clapper, J.D., et al., *Development and characterization of photopolymerizable biodegradable materials from PEG-PLA-PEG block macromonomers.* Polymer, 2007. **48**(22): p. 6554-6564.
125. Yang, D.J., et al., *Fabrication and characterization of hydrophilic electrospun membranes made from the block copolymer of poly(ethylene glycol-co-wlactide).* Journal of Biomedical Materials Research Part A, 2007. **82A**(3): p. 680-688.
126. Junliang Yang, et al., *Nonisothermal crystallization behavior of the poly(ethylene glycol) block in poly(L-lactide)-poly(ethylene glycol) diblock copolymers: Effect of the poly(L-lactide) block length.* Journal of Polymer Science Part B: Polymer Physics, 2006. **44**(22): p. 3215-3226.
127. Xu, X.L., et al., *The release behavior of doxorubicin hydrochloride from medicated fibers prepared by emulsion-electrospinning.* European Journal of Pharmaceutics and Biopharmaceutics, 2008. **70**(1): p. 165-170.
128. Jiang, H.L., et al., *Preparation and characterization of ibuprofen-loaded poly(lactide-co-glycolide)/poly(ethylene glycol)-g-chitosan electrospun membranes.* Journal of Biomaterials Science-Polymer Edition, 2004. **15**(3): p. 279-296.
129. Romero-Cano, M.S. and B. Vincent, *Controlled release of 4-nitroanisole from poly(lactic acid) nanoparticles.* Journal of Controlled Release, 2002. **82**(1): p. 127-135.
130. Langer, R. and N.A. Peppas, *Advances in biomaterials, drug delivery, and bionanotechnology.* Aiche Journal, 2003. **49**(12): p. 2990-3006.

131. Xiuling, X., et al., *Preparation of Core-Sheath Composite Nanofibers by Emulsion Electrospinning.* Macromolecular Rapid Communications, 2006. **27**(19): p. 1637-1642.
132. Katti, D.S., et al., *Bioresorbable nanofiber-based systems for wound healing and drug delivery: Optimization of fabrication parameters.* Journal of Biomedical Materials Research Part B-Applied Biomaterials, 2004. **70B**(2): p. 286-296.
133. Kim, K., et al., *Incorporation and controlled release of a hydrophilic antibiotic using poly(lactide-co-glycolide)-based electrospun nanofibrous scaffolds.* Journal of Controlled Release, 2004. **98**(1): p. 47-56.
134. Koh, H.S., et al., *Enhancement of neurite outgrowth using nano-structured scaffolds coupled with laminin.* Biomaterials, 2008. **29**(26): p. 3574-3582.
135. Ma, Z. and S. Ramakrishna, *Electrospun regenerated cellulose nanofiber affinity membrane functionalized with protein A/G for IgG purification.* Journal of Membrane Science, 2008. **319**(1-2): p. 23-28.
136. Ahmed, I., et al., *Three-dimensional nanofibrillar surfaces covalently modified with tenascin-C-derived peptides enhance neuronal growth in vitro.* Journal of Biomedical Materials Research Part A, 2006. **76A**(4): p. 851-860.
137. Choi, J.S. and H.S. Yoo, *Electrospun nanofibers surface-modified with fluorescent proteins.* Journal of Bioactive and Compatible Polymers, 2007. **22**(5): p. 508-524.
138. Jia, J., et al., *Preparation and immobilization of soluble eggshell membrane protein on the electrospun nanofibers to enhance cell adhesion and growth.* Journal of Biomedical Materials Research Part A, 2008. **86A**(2): p. 364-373.
139. Casper, C.L., et al., *Coating electrospun collagen and gelatin fibers with perlecan domain I for increased growth factor binding.* Biomacromolecules, 2007. **8**(4): p. 1116-1123.
140. Ki, T.G. and T.G. Park, *Biomimicking extracellular matrix: Cell adhesive RGD peptide modified electrospun poly(D, L-lactic-co-glycolic acid) nanofiber mesh.* Tissue Engineering, 2006. **12**(4): p. 1063-1063.
141. Huang, X.J., et al., *Electrospun nanofibers modified with phospholipid moieties for enzyme immobilization.* Macromolecular Rapid Communications, 2006. **27**(16): p. 1341-1345.
142. Dirk Grafahrend, et al., *Control of protein adsorption on functionalized electrospun fibers.* Biotechnology and Bioengineering, 2008. **101**(3): p. 609-621.
143. Ainslie, K.M., et al., *Cell adhesion on nanofibrous polytetrafluoroethylene (nPTFE).* Langmuir, 2007. **23**(2): p. 747-754.
144. Kim, G., et al., *Fabrication of a biocomposite reinforced with hydrophilic eggshell proteins.* Biomedical Materials, 2007. **2**(4): p. 250-256.
145. Wang, W., et al., *Influences of mechanical properties and permeability on chitosan nano/microfiber mesh tubes as a scaffold for nerve regeneration.* Journal of Biomedical Materials Research Part A, 2008. **84A**(2): p. 557-566.
146. Meiners, S., et al., *Engineering electrospun nanofibrillar surfaces for spinal cord repair: a discussion.* Polymer International, 2007. **56**(11): p. 1340-1348.

147. Grafahrend, D., et al., *Biofunctionalized poly(ethylene glycol)-block-poly(epsilon-caprolactone) nanofibers for tissue engineering.* Journal of Materials Science-Materials in Medicine, 2008. **19**(4): p. 1479-1484.
148. Prabhakaran, M.P., et al., *Surface modified electrospun nanofibrous scaffolds for nerve tissue engineering.* Nanotechnology, 2008. **19**(45): p. -.
149. Wen, X.T., et al., *Preparation of electrospun PLA nanofiber scaffold and the evaluation in vitro.* Asbm6: Advanced Biomaterials Vi, 2005. **288-289**: p. 139-142.
150. Chua, K.N., et al., *Stable immobilization of rat hepatocyte spheroids on galactosylated nanofiber scaffold.* Biomaterials, 2005. **26**(15): p. 2537-2547.
151. Sanders, E.H., et al., *Two-phase electrospinning from a single electrified jet: Microencapsulation of aqueous reservoirs in poly(ethylene-co-vinyl acetate) fibers.* Macromolecules, 2003. **36**(11): p. 3803-3805.
152. Tadmor, R., *Line Energy and the Relation between Advancing, Receding, and Young Contact Angles.* Langmuir, 2004. **20**(18): p. 7659-7664.
153. Israelachvili, J., *Intermolecular and Surface Forces*. 1985: Academic Press.
154. Krevelen, D.W.V., *Properties of Polymers*. 2nd revised edition ed. 1976: Elsevier Scientific Publishing Company.
155. Renate Förch, Holger Schönherr, and A.T.A. Jenkins, *Surface design: applications in bioscience and nanotechnology*. 2009: Wiley-VCH.
156. Clegg, C. *How to Measure a Contact Angle with DROPimage* Apr 1, 2009 [cited; Available from: http://knol.google.com/k/how-to-measure-contact-angle#.
157. Taek Gyoung Kim and T.G. Park, *Biomimicking extracellular matrix: cell adhesive RGD peptide modified electrospun poly(D,L-lactic-co-glycolic acid) nanofiber mesh.* Tissue Eng, 2006. **12**(2): p. 221-233.
158. Robert, L. and A.P. Nicholas, *Advances in biomaterials, drug delivery, and bionanotechnology.* AIChE Journal, 2003. **49**(12): p. 2990-3006.
159. Xu, X., et al., *Ultrafine medicated fibers electrospun from W/O emulsions.* Journal of Controlled Release, 2005. **108**(1): p. 33-42.
160. Xiuling Xu, Shufei Zhou, and W. Zhong, *Electrospun PEG-PLA nanofibrous membrane for sustained release of hydrophilic antibiotics.* Journal of Applied Polymer Science, in press, 2009.
161. Srikar, R., et al., *Desorption-Limited Mechanism of Release from Polymer Nanofibers.* Langmuir, 2007. **24**(3): p. 965-974.
162. Siparsky, G.L., K.J. Voorhees, and F.D. Miao, *Hydrolysis of polylactic acid (PLA) and polycaprolactone (PCL) in aqueous acetonitrile solutions: Autocatalysis.* Journal of Environmental Polymer Degradation, 1998. **6**(1): p. 31-41.